AN EXPERIMENTAL STUDY OF A STRUCTURAL CONCRETE DEEP BEAM WITH A LARGE OPENING USING THE STRUT-AND-TIE MODEL

by

Brian Scott Maxwell, BSCE

DEPARTMENTAL REPORT

Presented to the Faculty of the Civil Engineering Department of

The University of Texas at Austin

in Partial Fulfillment

of the Requirements

for the Degree of

MASTER OF SCIENCE IN ENGINEERING

THE UNIVERSITY OF TEXAS AT AUSTIN

December 1996

AN EXPERIMENTAL STUDY OF A STRUCTURAL CONCRETE DEEP BEAM WITH A LARGE OPENING USING THE STRUT-AND-TIE MODEL

APPROVED BY

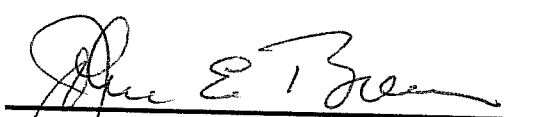

John E. Breen

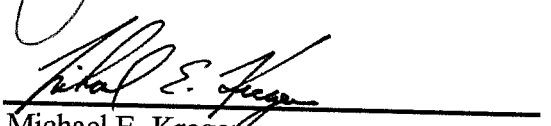

Michael E. Kreger

To my parents.

ACKNOWLEDGEMENTS

The research described in this thesis was conducted at the Phil M. Ferguson Structural Engineering Laboratory of the University of Texas at Austin by the author under the supervision of Dr. John E. Breen.

The author is greatly indebted to Dr. John E. Breen for his continuous and invaluable guidance and support as teacher, supervisor, and friend. No part of this report would have been possible without his assistance. Likewise, the author wishes to express his gratitude to Dr. Michael E. Kreger for his comments and suggestions. Assistance from the staff of Ferguson Lab is gratefully acknowledged as well.

Additional and sincere thanks go to Kevin Clinch and my brother Craig Maxwell. Without their help, my life would have been greatly complicated.

Brian Scott Maxwell
December 6, 1996
Austin, Texas

ABSTRACT

AN EXPERIMENTAL STUDY OF A STRUCTURAL CONCRETE DEEP BEAM WITH A LARGE OPENING USING THE STRUT-AND-TIE MODEL

by

Brian Scott Maxwell, BSCE

The University of Texas at Austin, 1996

SUPERVISOR: John E. Breen

Where geometric discontinuities exist in structural concrete members, current code documents provide little direction for design. A greater understanding of how to design a reinforced concrete deep beam with a geometric discontinuity in the form of a large opening can be obtained by using strut-and-tie models. Combinations of two distinctly different strut-and-tie models were used to design four specimens. Physical models were constructed using sack concrete and 3-mm and 6-mm reinforcing bars. The development lengths for the small bars were determined using a method developed by Ferguson at The University of Texas. The deep beams were simply supported and tested using a point load. Each of the four beams resisted considerably more than the factored design load. This successful test series reveals the power, versatility, reliability, and predictability of the strut-and-tie modeling technique.

TABLE OF CONTENTS

CHAPTER 4

CHAPTER 5

CHAPTER 8

CHAPTER 9

LIST OF FIGURES

PAGE

LIST OF TABLES

PAGE

CHAPTER 1

INTRODUCTION

1.1. General

Current code documents such as the ACI Committee 318-95 Building Code (1995) govern how structural concrete is to be constructed and designed. The ACI Building Code gives a thorough understanding of design and construction requirements for standard and commonly used members. If, however, a nonstandard or unusual member is advantageous or necessary, such as a member having a statical or geometric discontinuity, the ACI Building Code gives little if any guidance. Such discontinuities can take the form of frame corners, corbels, recesses, and large openings. These unusual members are usually combinations of standard members connected by areas of transition. These transition areas require special attention.

Thus, the problem reveals itself. How are these unusual members with such discontinuities to be consistently and safely designed? A possible solution consists of generalizing the well known truss analogy which has been used quite successfully where beams in combined flexure, shear, and torsion are concerned. By generalizing the truss analogy into strut-and-tie models, the appropriate approach can be found for designing unusual structural concrete members (Schlaich et al., 1987).

A landmark paper was published on this concept in a 1987 *PCI Journal* article by Jörg Schlaich, Kurt Schäfer, and Mattias Jennewein. Their paper, "shows how suitable strut-and-tie models are developed and proposes criteria according to which the model's elements can

be dimensioned uniformly for all possible cases." The paper includes a number of numerical design examples of unusual reinforced concrete and prestressed concrete members.

This excellent paper by Schlaich et al. introduces the strut-and-tie modeling technique by illustrating how to choose and design an appropriate strut-and-tie model. The paper shows how to translate the strut-and-tie model into a layout of necessary reinforcing steel. Schlaich et al. demonstrate how the strut-and-tie model gives an appropriate mechanism to resist the stresses developed in a member. One of the designs in the Schlaich paper is a deep beam with a geometric discontinuity. A large opening is placed in the corner of a simply supported deep beam which carries a concentrated load as shown in Figure 1-1. How then to place the reinforcing bars in the beam to allow the load to flow around the hole to the support? Schlaich et al. develop a theoretical strut-and-tie model for this deep beam with a large opening and design the required reinforcement patterns for construction.

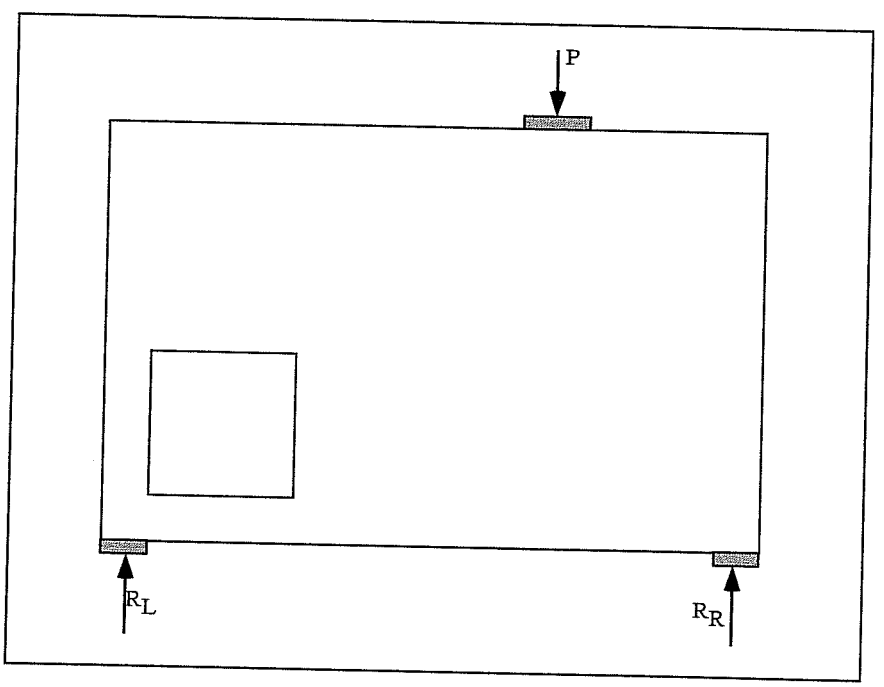

Figure 1-1 - Deep Beam Test Specimen

1.2. Objective

The objective of this investigation is to verify the basic concepts of strut-and-tie modeling and its applicability and versatility by physically testing the performance of a deep beam with a large opening designed using the strut-and-tie model approach presented by Schlaich et al. The numerical example given by Schlaich et al. starts with an elastic finite element model of the beam and a choice of two strut-and-tie models used in combination to resist the specified loading. This investigation uses the two strut-and-tie models in various combinations and with some supplementation to design four specimens. Models of the four specimens were constructed, loaded to failure, and the performance of the four specimens was evaluated.

1.3. Scope

The four specimens that were constructed were based on the strut-and-tie model suggested by Schlaich et al. and included a scaled version of their example. The model specimens were constructed using sack concrete and 3-mm and 6-mm reinforcing bars. This report documents the process of designing an appropriate concrete mix for the scaled models, determining development lengths of the small reinforcement in the microconcrete, as well as the design, construction, and testing of the strut-and-tie model specimens. It concludes with an evaluation of the test results and strut-and-tie model usage in general.

1.4. Outline of the Report

Chapter 2 presents background data relevant to the experiment and introduces the strut-and-tie model. Related research is noted and necessary scaling concepts are also

presented in Chapter 2. The unique materials used for construction of the models are discussed in Chapter 3. Chapter 4 deals with the determination of the development length for the small 3-mm and 6-mm reinforcing bars in the microconcrete using a test method developed by Prof. Phil M. Ferguson at The University of Texas. Analysis and design of each of the four specimens is presented in Chapter 5. Experimental procedures are covered in Chapter 6 including a description of the testing setup and instrumentation. Chapter 7 presents all test results for each specimen. This is where failure patterns and cracking patterns are presented along with numerical data. The analytical and experimental results are discussed in Chapter 8. Finally, Chapter 9 presents conclusions and summaries with a look at future developments and research needed.

CHAPTER 2

BACKGROUND

2.1. Strut-and-Tie Model Basics

For the design of structural concrete, the strut-and-tie model gives the designer a transparent and consistent solution. In general, reinforced concrete members consist of compressive stress fields which are distributed and interconnected by tensile ties (Schlaich et al., 1987). This conceptual model makes visualizing the flow of forces within a structure easy, and allows for the proper proportioning of reinforcement (Bergmeister et al., 1993). The basic idea of the strut-and-tie model is to design a truss mechanism where all stresses are condensed into compression and tension members connected by nodes. The compression stresses are carried by the concrete and tensile stresses are resisted by reinforcing bars. Thus, the first step in the design of a member using the strut-and-tie model is to determine the stress distribution that is developed due to loading and support conditions.

If the structural member to be designed presents a complex or unfamiliar stress distribution, an elastic finite element analysis can be used to give the designer an idea of force distributions within the uncracked member. The finite element solution also provides general patterns of major tension fields. This elastic stress distribution will suggest how and where the struts and ties of the model should be designed and oriented.

Most structural concrete members are composed of two distinct types of regions classified as D-(Discontinuity) and B-(Bending) regions (Bergmeister et al., 1993). The B-regions are areas where plane sections remain plane. These regions can be designed by analyzing the sectional forces and using traditional methods. In the D-regions, nonlinear strain

distributions exist due to statical or geometrical discontinuities (Bergmeister et al., 1993). Examples of a number of D-regions are shown in Figure 2-1. Thus, the overall structure is designed most efficiently by using traditional methods for the design of the B-regions, determining the forces imposed on the D-regions by the B-regions, and using the strut-and-tie model to design the D-regions.

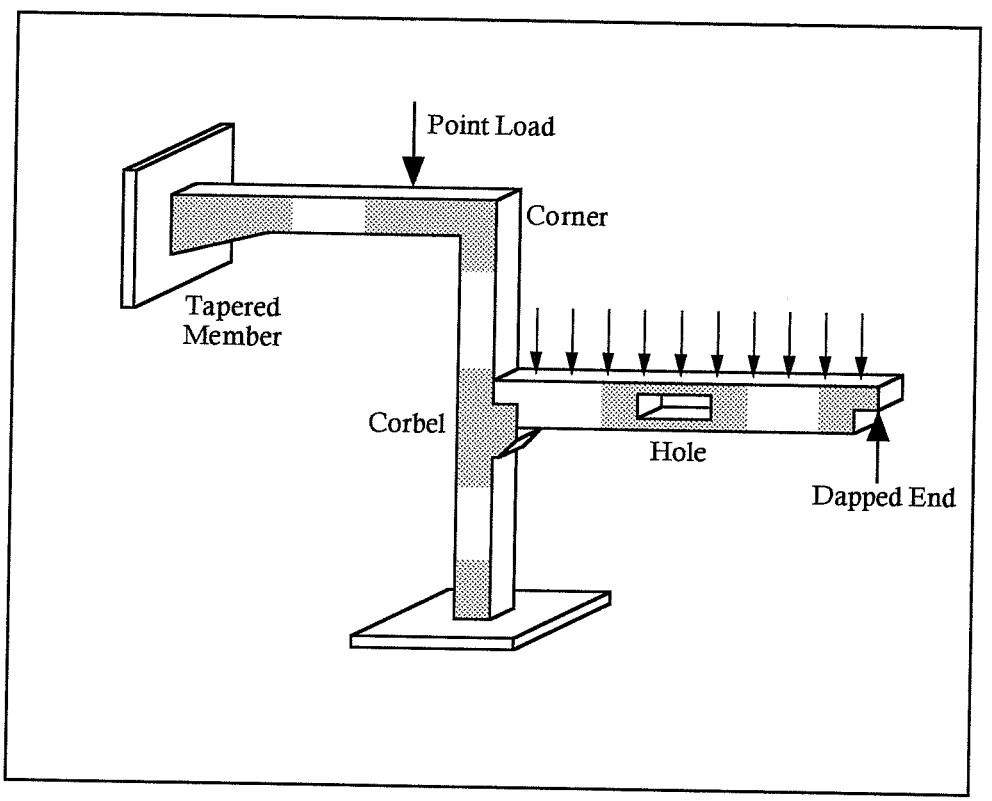

Figure 2-1 - Example of D-Regions (shown shaded) (Bergmeister et al., 1993)

For any particular stress distribution, there can be a number of different strut-and-tie models developed. Some may be more logical than others, but all patterns should be sufficient, provided the designer has accounted for all stresses in the member. The structure adapts itself to the assumed internal structural system (Schlaich et al., 1987). The strut-and-

tie model is a lower-bound plasticity solution yielding conservative results (Bergmeister et al., 1993).

Once the appropriate strut-and-tie model or combination of strut-and-tie models are chosen, the forces in each component can be simply determined by analysis. It is then necessary to dimension struts, ties, and nodes. Sizing the reinforcement for the individual struts and ties is an important step in the design, but it is equally important to check the nodes for the ability to transfer loads between the struts and ties. Thus, it is necessary to design compression concrete struts, tension ties, and a possibility of four node types. Node types consist of combinations of struts, C, and ties, T. The nodes can have three compression struts (CCC-nodes), two struts and one tie (CCT-nodes), one strut and two ties (CTT-nodes), or three ties (TTT-nodes) (Schlaich et al., 1987). Examples of these node types are shown in Figure 2-2. It is important to design the nodes so that proper reinforcement anchorage is provided and compression stresses in the concrete are below the acceptable limit.

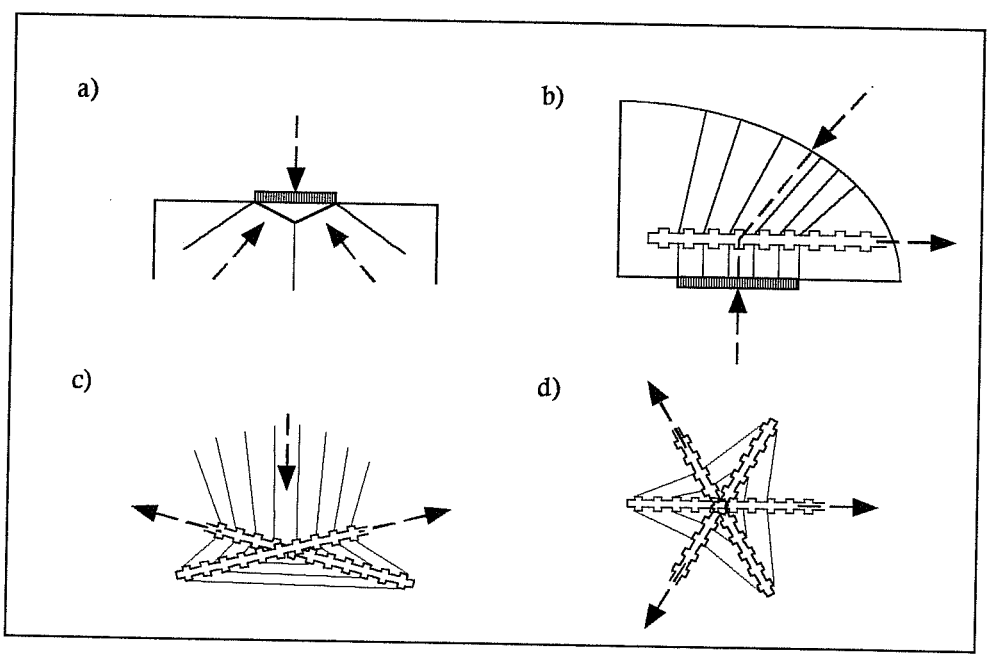

Figure 2-2 - Examples of Node Types: a) CCC-node, b) CCT-node, c) CTT-node, d) TTT-node (Schlaich et al., 1987)

Through the preceding process, the strut-and-tie model provides a consistent method for determining where reinforcing bars need to be located within a member which would otherwise be designed using "past experience" or "common knowledge," and, while the plasticity theory behind the strut-and-tie model is complex, the process of using the strut-and-tie model is quite simple and straight forward (Schlaich et al.,1987).

2.2. Reason for Using the Strut-and-Tie Model

For this investigation, the strut-and-tie model is the only solution that gives a consistent design of the deep beam with a large opening. The large opening causes the beam to become essentially one D-region. Traditional methods are unable to address the design around the geometric discontinuity. The transparent solution presented by the strut-and-tie model allows for a simple and rather quick design of reinforcement and placement in the deep beam. All internal stresses are accounted for, and, since the strut-and-tie model is a lower-bound solution, the resulting design should be a conservative and useful solution.

2.3. Related and Past Research

First and foremost, the paper entitled "Toward a Consistent Design of Structural Concrete" written by Jörg Schlaich, Kurt Schäfer, and Mattias Jennewein and published in 1987 by the *PCI Journal* is of primary influence in this investigation and report. The journal article is based on the investigation and work done by the authors at the University of Stuttgart in Germany. Much of the work presented in the *PCI Journal* was previously reported in the German language for the Comité Euro-International du Béton and the German Betonkalender (Schlaich et al., 1987). The article presents the ideas of the strut-and-tie model

as well as a large number of applications for both reinforced concrete and prestressed concrete members.

Other research of strut-and-tie modeling is presented in a report from the Center for Transportation Research at The University of Texas at Austin (Bergmeister et al., 1993). This report is based on research conducted for the Texas Department of Transportation and is entitled "Detailing for Structural Concrete" by Konrad Bergmeister, John E. Breen, James O. Jirsa, and Michael E. Kreger. The reader is encouraged to refer to this report for a complete history and evolution of the strut-and-tie model. The report also gives a number of applications of the strut-and-tie model and provides a number of design aids for anyone interested in such techniques.

Since the intent of this report is to examine the feasibility of the strut-and-tie model for one particular case, a thorough investigation of the history and evolution of the technique is not presented. Also, an in-depth analysis of design solutions for a number of different members is left to the two previous articles mentioned. The reader is encouraged to read the two reports in an attempt to obtain an overall understanding of the strut-and-tie model process.

2.4. Scaling

The four constructed specimens are scale models based upon a design done by Schlaich et al. Loading capacity, cost, and time limitations precluded the use of full scale prototypes of the deep beams. Thus, a direct scaling method was used to reduce the beams to a size practical for the scope of this project. The "direct" scaling method uses a true-to-scale

model which represents the actual structure (Aldridge, 1966). This method of scaling is preferred when studying the response of concrete structures loaded to collapse.

The background and derivation of such direct modeling is presented in a dissertation written by Weldon W. Aldridge entitled "Ultimate Tests of Model Reinforced Concrete Folded Plate Structures." In his dissertation, Aldridge details tests performed on a number of scaled models representing reinforced concrete folded plate structures. Most of the following information is credited to his work.

By using the direct method of scaling, all dimensions of the full scale member are reduced by a scale factor. For its use in this report, it is necessary to include two similarities between the actual member and the model. There needs to exist a geometric and mechanical similarity. The geometric similarity exists when using the constant scaling factor. Mechanical similarity is more complicated to achieve and Aldridge presents the derivation. Using this derivation, the geometric dimensions of the actual member were scaled by a factor, f, while the concentrated load was scaled by a factor of f^2.

Thus, for the purpose of this project, all dimensions of the actual member were multiplied by a scaling factor of 1/5.5, whereas the load was multiplied by a factor of 1/30.25. Aldridge showed that in this way, the similarity between the actual structure and the model will be maintained.

CHAPTER 3

MATERIALS

3.1. Scaled Materials

As discussed in Chapter 2, the constructed specimens were scale models of the deep beam designed by Schlaich et al. Due to this scaling, materials used to construct the specimens had to be of appropriate scale. Thus, a microconcrete containing pea gravel and small steel reinforcement bars were used for construction. This chapter explains the properties and performance of these two materials.

3.2. Microconcrete

For the construction of the specimens, pre-bagged concrete mix was used. The concrete mix was combined with water and a superplasticizer to yield concrete with a design compressive strength of 4000-psi. The superplasticizer is a high range, water reducing admixture and was added to increase the strength of the concrete by reducing the amount of water required in the mix. These ingredients were used to make two batches of concrete at different times. The first batch was used to cast the development length specimens and 3"X 6" cylinders. The cylinders were used to monitor the strength gain of the mix to determine if the proposed mix would be proper for the tests. The second batch was mixed weeks later and was used to cast the actual specimens. Again, 3"X 6" cylinders were cast to determine the strength of the concrete in the specimens. Such cylinder tests allowed for an examination of the strength gain of the concrete over a 28-day period.

3.1.1. Mix Properties

The concrete used had three main ingredients: sacks of pre-blended concrete mix, water, and superplasticizer. Eighty pound sacks of concrete mix were used as the main ingredient. Each eighty pound sack consisted of 13-lbs. of cement, 33.5-lbs. of sand, and 33.5-lbs. of pea gravel (Waxler, 3 June 1996). The superplasticizer was added to reduce the amount of water and thus increase the strength of the concrete. Water was added to the mix to achieve a water-to-cement ratio of 0.6 by weight. The amount of material used for 1.2-cubic feet of concrete is given in Table 3-1.

Table 3-1 - Microconcrete Mix

INGEDIENTS FOR 1.2 CU. FT. OF CONCRETE
2 - 80 lb. sacks of concrete mix
4 fl. oz. superplasticizer
15.5 lbs. water

3.3.2. Strength Properties

The performance of the concrete used for the specimens was monitored in a number of ways. Part of the first batch of concrete, which was used for the development length specimens, was cast into 3"X 6" cylinders. These cylinders were tested for compressive strength at 3, 7, 14, 21, and 28 days. The second batch of concrete was used for casting the main specimens. Again, 3"X 6" specimens were cast and tested at 7, 14, and 21 days. Finally, after testing, two inch diameter specimens were cored out of the actual deep beams. These core samples gave a good idea of the 28-day compressive strength of the specimens.

Table 3-2 - Microconcrete Strength Properties

CONCRETE STRENGTH PROPERTIES							
Age (days)	1st Batch Ult. Load (lb.)	1st Batch f'c (psi.)	Actual Mix Ult. Load (lb.)	Actual Mix f'c (psi.)	Cored Samples Ult. Load (lb.)	Cored Samples f'c (psi.)	Average f'c (psi.)
0	0	0	0	0	0	0	0
3	11700	1660					
	12400	1750					1700
7	19500	2760	22750	3220			
	19380	2740					2910
14	24400	3450	25880	3660			
	25320	3580					3560
21	30030	4250	28950	4100			
	29250	4140					4160
28	35600	5040			*2" Cored Samples*		
	36130	5110			12960	4130	
					13220	4210	
					12580	4000	
	3"X 6" Cylinder Samples				12660	4030	
					12720	4050	
					12670	4030	
					12990	4130	
					13150	4190	4290

SPLIT CYLINDER PROPERTIES

@14 days: fct =	427 psi.	
	434 psi.	Average fct
@21 days: fct =	418 psi.	
	408 psi.	405 psi.
	387 psi.	
	354 psi.	

Split cylinder tests were also used to determine the tensile strength of the concrete. All results from the compressive and split cylinder tests are presented in Table 3-2.

Table 3-2 shows all of the cored concrete specimens having a compressive strength near the targeted value of f'_c = 4000-psi. The last column averages the concrete strengths for each age and these average concrete strengths are plotted in Figure 3-1. This plot shows all of the specimens plotted as different points with a curve drawn through the average values for each age. Of importance also is the fact that the split cylinder strengths are near the accepted value of $\bar{f}_{ct} \approx 6.4\sqrt{f'_c}$ where $\bar{f}_{ct}$ is the split cylinder strength in psi., and f'_c is the compressive strength in psi.

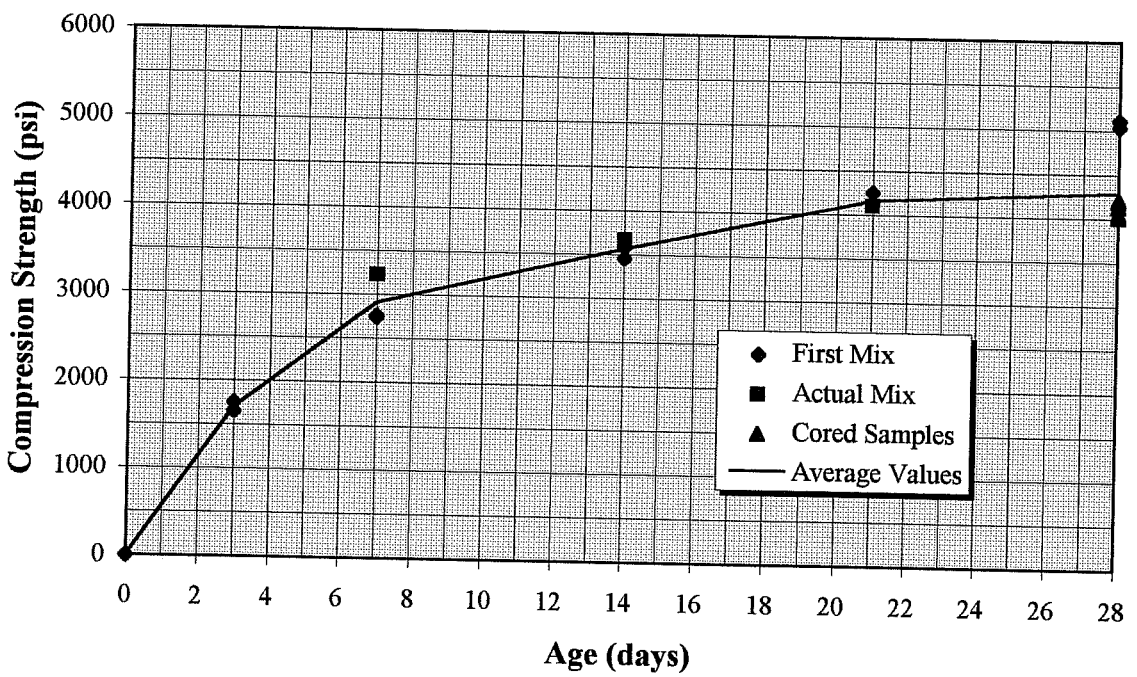

Figure 3-1 - Microconcrete Strength Curve

3.3. Steel Reinforcing Bar

The steel reinforcing bars used for construction were small deformed bars. The deep beam model reinforcement cages were constructed using both 3-mm and 6-mm diameter bars.

Originally, three different sized bars were obtained for possible use in the specimens, 3-mm, 4-mm, and 6-mm bars. Data for all three bars are shown in this section even though the 4-mm bar was not used in the actual specimens. Development lengths were determined for all three bar sizes.

Table 3-3 shows the properties of the steel used. The strength of the reinforcement was obtained from tension tests of bar coupons. Table 3-3 lists an assumed diameter and an actual diameter. Each bar is referred to using the assumed diameter whereas the actual diameter was calculated by weighing a sample length of the bar, dividing by the unit weight of steel, and determining the diameter mathematically. The two values differ by some amount. The yield strength and design calculations are based on the actual diameter.

Table 3-3 - Steel Bars Used

STEEL REINFORCEMENT PROPERTIES				
Assumed Diameter (mm)	Actual Diameter (in)	Area (in^2)	Ultimate Load Pu (lb)	Yield Strength fy (ksi)
3	0.167	0.022	1880	85
4	0.185	0.027	2790	103
6	0.240	0.045	3690	82

If the yield strengths are examined from Table 3-3, there is a similarity in the yield strength between the 3-mm and 6-mm bars. For this reason, and since the actual area of the 3-mm bar is close to the actual area of the 4-mm bar, the main reinforcement cages for the deep beams were built using 3-mm and 6-mm bars only.

3.4. Conclusion

Thus, the materials used in this project are established. The ingredients of the microconcrete mix are determined and provide positive results with a consistent compressive strength of 4000-psi. The properties of the steel reinforcing bar are shown along with an explanation of which bars are used in the specimens. The next step is to determine the necessary development length of the small bars in the microconcrete. Chapter 4 will expand on this topic.

CHAPTER 4

DEVELOPMENT LENGTH TESTS

4.1. Test Beams

As mentioned earlier, the deep beams that were constructed are scale models of full size beams. Most quantities can be directly scaled, yielding reasonable results as mentioned in Section 2.4. However, a problem arises when determining the development lengths of the small reinforcing bars. There is an inability to scale down design specifications for development lengths (Ferguson et al., 1988). This is most likely due to the increase in bond stresses that develop around small bars since the perimeter varies linearly with the scale but the bar area (and hence tensile force) varies with the square of the scale. Another problem exists because, while the results or specimens are scaled down, the crack size in the concrete does not always scale. Thus, it was necessary to use the microconcrete to determine the development length required to develop the full tensile capacity of the small deformed bars.

For the purpose of determining the development length of the small bars, test beam specimen design and loading arrangement were used that were developed by Prof. Phil M. Ferguson at The University of Texas. Prof. Ferguson developed a simple span test beam with a cantilever overhang which allows for the development length of the bar to be tested in the negative moment region of the beam. This specimen can be seen in Figure 4-1. The maximum steel stress and average bond stress can be calculated from this test. This particular type of development length specimen was approved by ACI Committee 208 Bond Stress in 1958 (Ferguson and Thompson, 1962). The advantage of this test beam is that it permits the tested bar to be an isolated portion of the negative moment steel allowing the test bar to be

independent of neighboring bars, reactions, and load points thus giving the simplest attainable bond conditions along the length (Ferguson and Thompson, 1962). These tests also give a realistic measure of the development lengths because in actual structures the bond stress and development length cannot be isolated from diagonal tension and flexural stresses.

These test beams were used in a series of tests done by Prof. Ferguson and Prof. J. Neils Thompson. They presented their findings in *The Journal of The American Concrete Institute* in July 1962 in an article entitled "Development Length of High Strength Reinforcing Bars in Bond." A great number of tests were performed, some of which tested development lengths equal to 18 and 24 bar diameters. It was decided that it would be necessary to determine the development length of the small reinforcing bars used in this experiment (3-mm, 4-mm, and 6-mm). Two test beams were constructed for each bar size. One had a development length of 18 bar diameters, while the other had a development length of 24 bar diameters. The beams were tested to failure and the maximum steel stress was calculated. Thus, from this set of specimens, a graph was generated showing steel stress as a function of development length. This allowed for the use of the correct development length, knowing the desired steel stress.

4.2. Design of the Test Specimens

Six specimens were constructed and tested to obtain curves which would give the needed development length for the desired steel stress. The test beam is shown in Figure 4-1. The variables are different for each specimen and are defined in Table 4-1. These dimensions are scaled directly from Ferguson's tests. The closely spaced stirrups in the cantilever region of the beam force the failure to occur along the development length of the test bar.

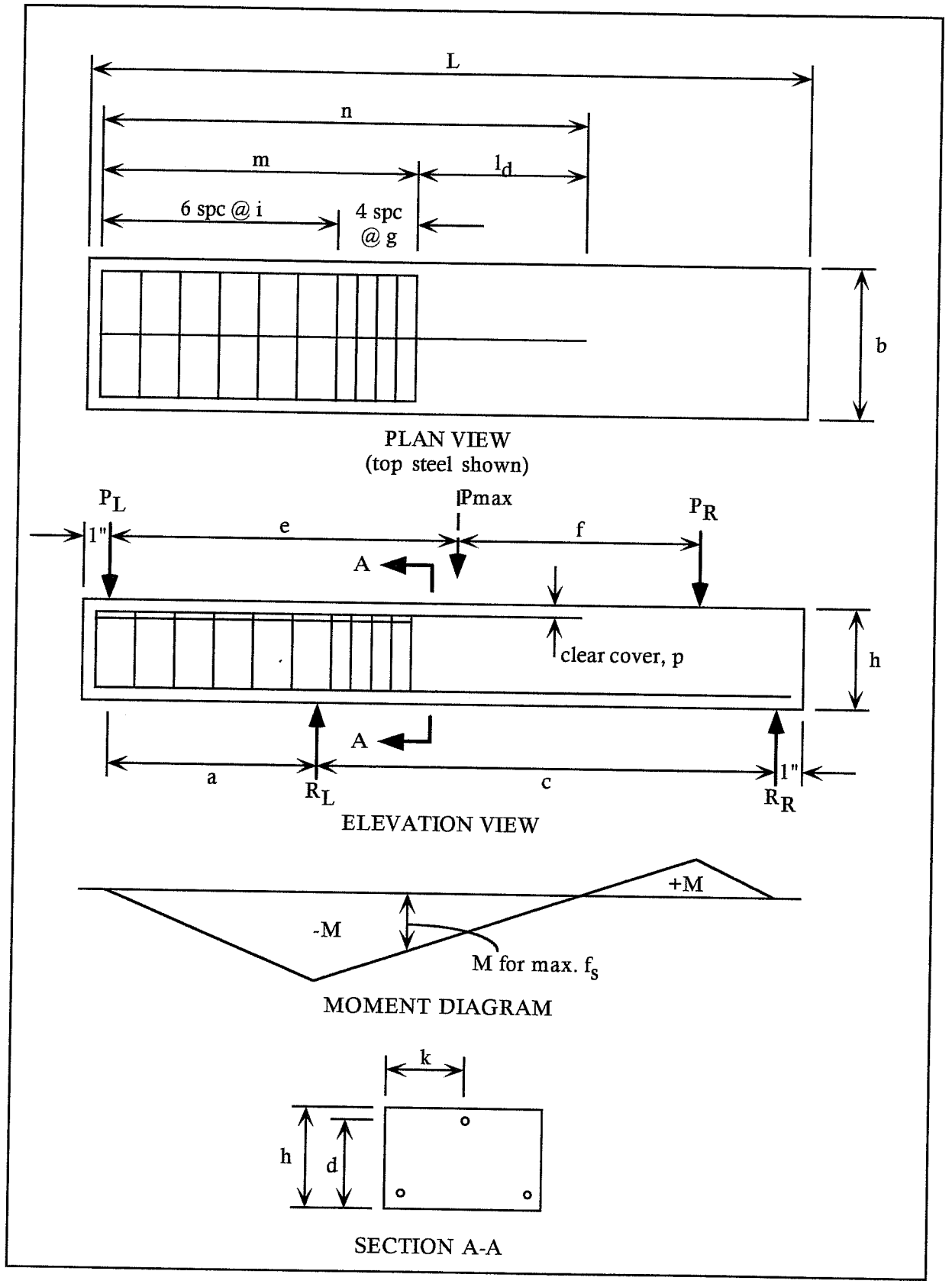

Figure 4-1 - Development Length Test Beam Dimensions

Table 4-1 - Development Length Test Beam Specifications

Specimen:		3-mm		4-mm		6-mm	
Development Length:		18D	24D	18D	24D	18D	24D
Dimensions:	a	3.0	3.0	4.5	4.5	6.5	6.5
(in.)	b	3.62	3.62	3.62	3.62	5.00	5.00
	c	9.0	9.0	11.5	11.5	17.5	17.5
	d	1.29	1.29	1.60	1.60	2.26	2.26
	e	5.5	5.5	7.5	7.5	10.75	10.75
	f	3.5	3.5	4.5	4.5	7.0	7.0
	g	0.3	0.3	0.4	0.4	0.5	0.5
	h	1.62	1.62	1.62	1.62	2.5	2.5
	i	0.5	0.5	0.75	0.75	1	1
	k	1.81	1.81	3.75	3.75	2.50	2.50
	L	13	13	18	18	26	26
	ld	2.1	2.8	2.8	3.8	4.3	5.7
	m	5.14	4.44	7.02	6.02	9.94	8.49
	n	7.24	7.24	9.82	9.82	14.19	14.19
	p	0.250	0.250	0.313	0.313	0.375	0.375

4.3. Testing

The test specimens were simply supported and loaded using a load distribution beam which distributed the point load of the machine to the desired two point loads on the specimen. This test setup can be seen in Figure 4-2. In this manner, the development length, l_d, was tested similarly to the way it is subjected to tension in a beam.

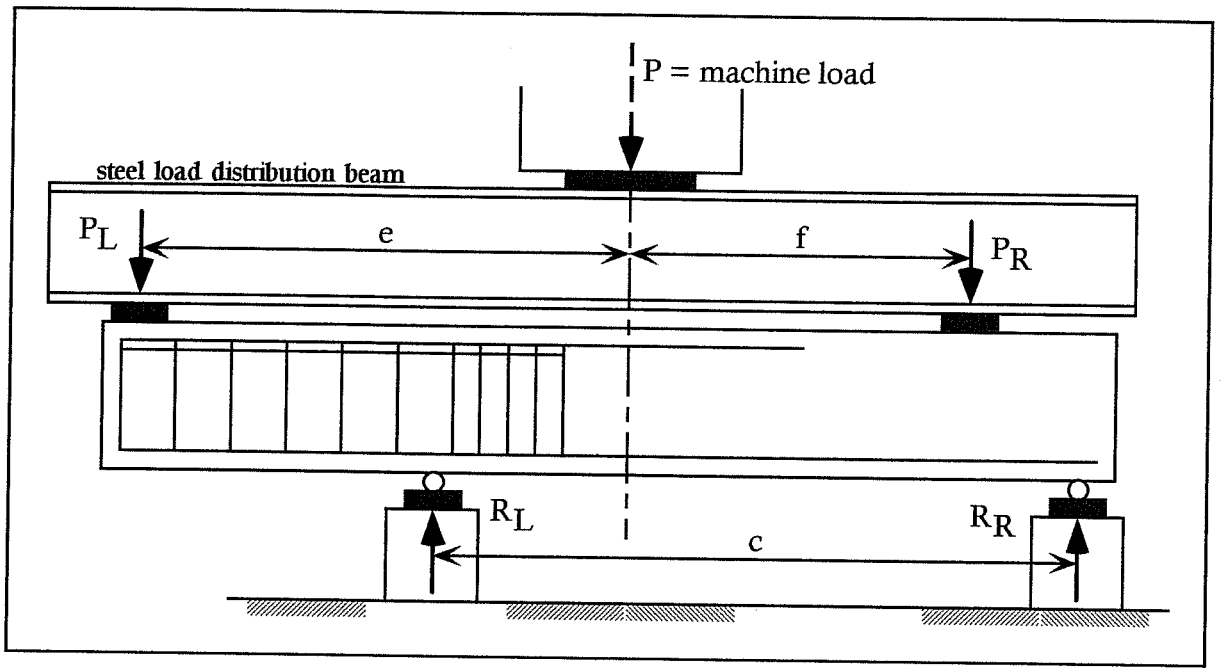

Figure 4-2 - Development Length Test Setup

4.4. Results

All of the specimens failed in a similar fashion. The typical failure pattern is shown on the unfolded top and side view given in Figure 4-3. This failure pattern shows diagonal tension (inclined side crack) with longitudinal splitting along and directly over the development length of the bar. By knowing the load when the beam failed, a moment diagram was constructed which visually gave the point of maximum moment at the critical point at the start of l_d and the associated steel stress in the tested bar. These values are given in Table 4-2. Each specimen provides a value for the maximum steel stress. These values are plotted in Figure 4-4 as a function of the l_d used. A linear interpolation of the two points for each bar is used giving a graph where, by knowing the steel yield stress, the required development length to fully develop yield, l_d, can be determined and is given in Table 4-3.

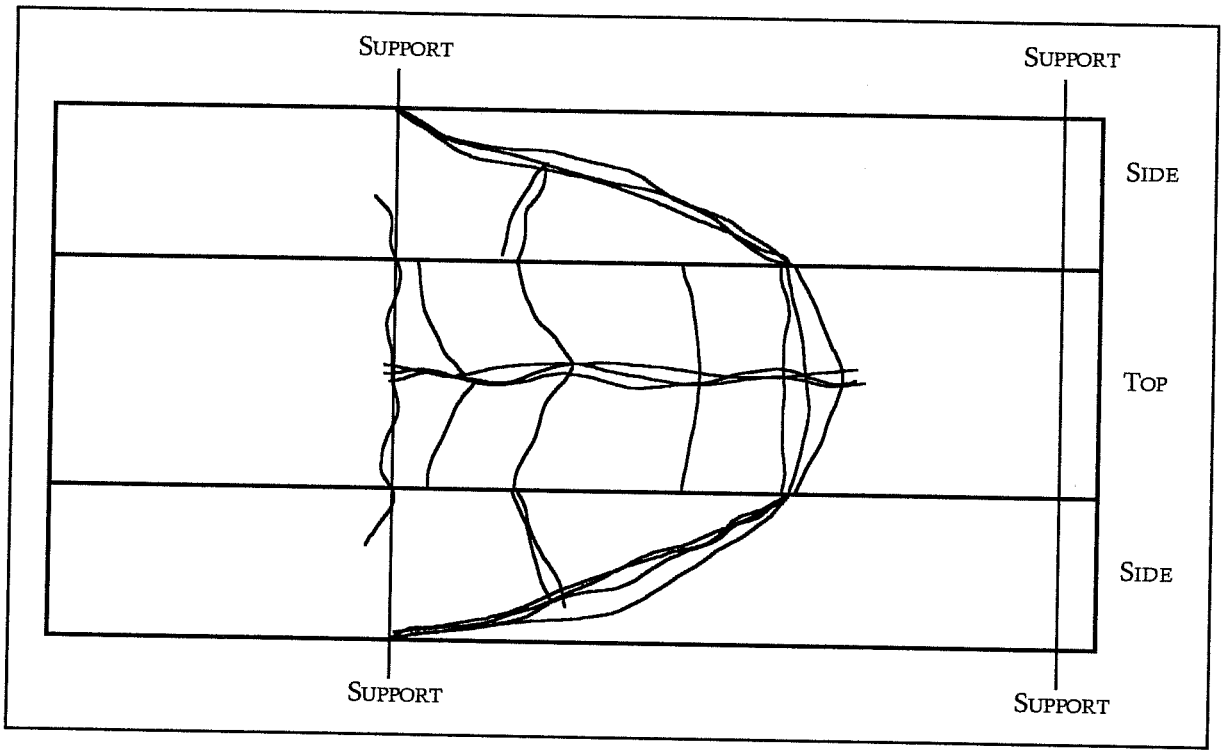

Figure 4-3 - Typical Crack Pattern for Development Length Specimen

Table 4-2 - Development Length Test Results

Specimen:		3-mm		4-mm		6-mm	
Development Length:		18D	24D	18D	24D	18D	24D
Pmax	(lbs.)	3260.0	3980.0	2600.0	2860.0	5100.0	5450.0
Pl	(lbs.)	1267.8	1547.8	975.0	1072.5	2009.4	2147.3
Pr	(lbs.)	1992.2	2432.2	1625.0	1787.5	3090.6	3302.7
Rl	(lbs.)	2354.5	2874.4	1921.4	2113.5	3860.7	4125.7
Rr	(lbs.)	905.5	1105.6	678.6	746.5	1239.3	1324.4
Mmax	(in.-lbs.)	2282.0	3715.0	2650.0	3960.0	7870.0	11280.0
fs	(ksi.)	89.3	145.4	68.2	101.7	86.2	123.5

Table 4-3 - Necessary Development Length

Specimen	fy (ksi.)	ld (in.)
3-mm	85	2.1
4-mm	103	3.8
6-mm	82	4.1

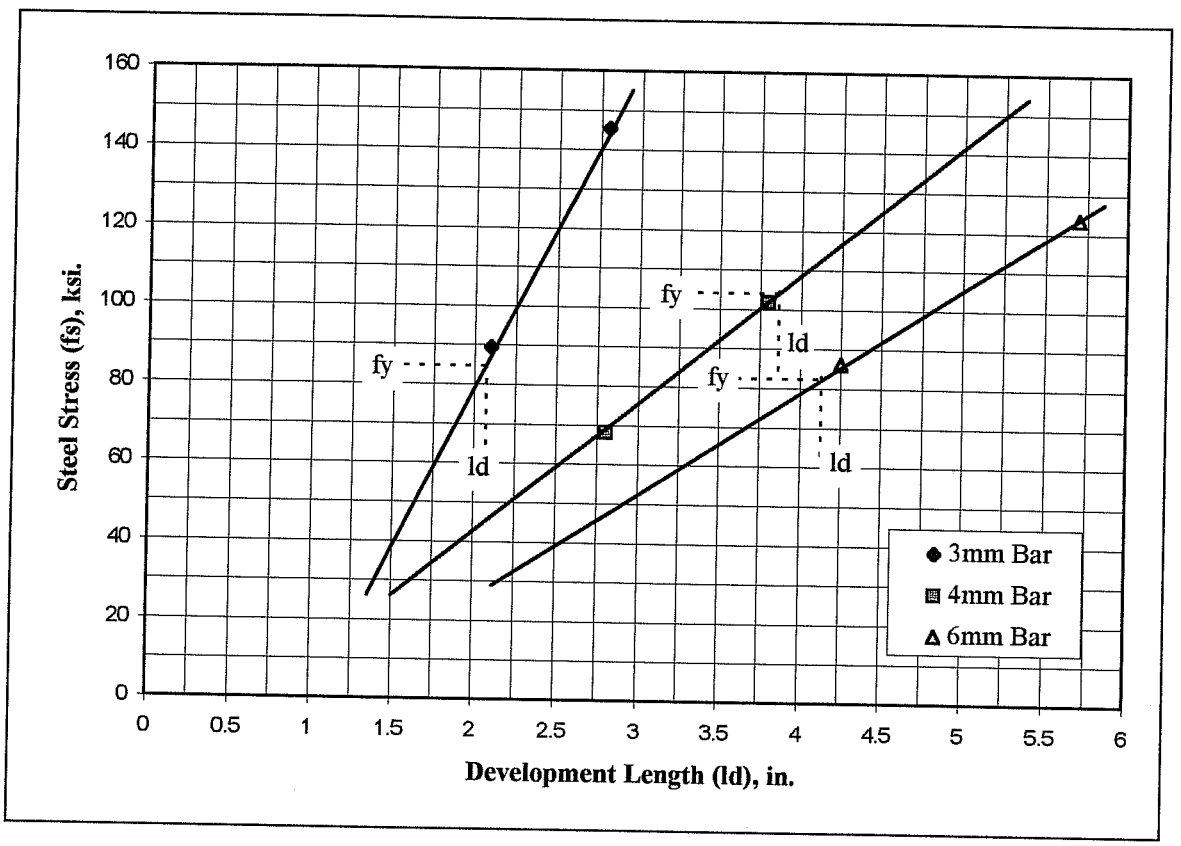

Figure 4-4 - Steel Stress vs. Development Length

4.5. Conclusions

The minimum development lengths determined from the graph of steel stress versus development length were used in the design of the deep beams with a large opening to ensure

all bars had sufficient anchorage so that they were properly developed. This allows the bars to develop full tensile capacity and not fail in bond. It should be emphasized that these test results are only valid for the bars with this project's particular type of concrete. No general scaling of development lengths is possible as previously pointed out.

CHAPTER 5

ANALYSIS AND DESIGN OF DEEP BEAM SPECIMENS

5.1. Deep Beam With a Large Opening

Attention is now turned to the design of the specimens that will be constructed to test the four strut-and-tie models. Schlaich et al. (1987) have provided the design of one deep beam specimen, and the designs presented here are variations of their original design. In their previously mentioned journal article entitled, "Toward a Consistent Design of Structural Concrete," Schlaich et al. present, as one of their many examples, the design of a deep beam with a large hole situated near one support. This model is included by Schlaich et al. because it shows how the strut-and-tie model is used to design a structure consisting mainly of one large D-region.

Schlaich et al. present a strut-and-tie model solution for the deep beam with a large opening by designing two different strut-and-tie models. They assume that the two strut-and-tie models each resist half of the applied load. Schlaich et al. state, "Each model in itself would be sufficient, but, looking at the elastic stresses, a combination of both appears to be better than either of them." The four specimens in this investigation are used to test this idea. The first specimen uses one of the strut-and-tie models designed by Schlaich et al., the second specimen uses the other strut-and-tie model, the third specimen uses the combination of the two strut-and-tie models as Schlaich et al. designed, and finally, the fourth specimen uses a variation of the third model which will be discussed later.

The deep beam designed by Schlaich et al. is a large member having a length of seven meters, height of approximately five meters, and a thickness of half a meter. This deep beam

is assumed to be subjected to a point load of three million newtons. As stated previously, this beam was scaled down to give the dimensions of the specimens in this investigation.

To scale the specimen, all dimensions were reduced using a factor of 5.5. This allows for geometric similarity to exist between the actual beam and the model. To maintain mechanical similarity, the concentrated load is scaled by the square of the scale factor, or 30.25. In this manner, the deep beam designed by Schlaich et al. is reduced to a smaller, more manageable size.

A distinction should be made to clarify the loading of the specimens. The beam is designed to withstand a factored concentrated load of 22-kips. To determine service loads, a value of ϕ=1 is assumed because the material strength is known, and ACI318-95 Building Code (1995) values for load factors are used assuming the dead load equals the live load. Thus, load factors for dead and live loads are averaged giving a load factor of 1.55. Using this load factor and ϕ value gives a service load of 14.6-kips. The model used for this investigation is shown in Figure 5-1. The first step in the design of the strut and tie model is the determination of D- and B-regions.

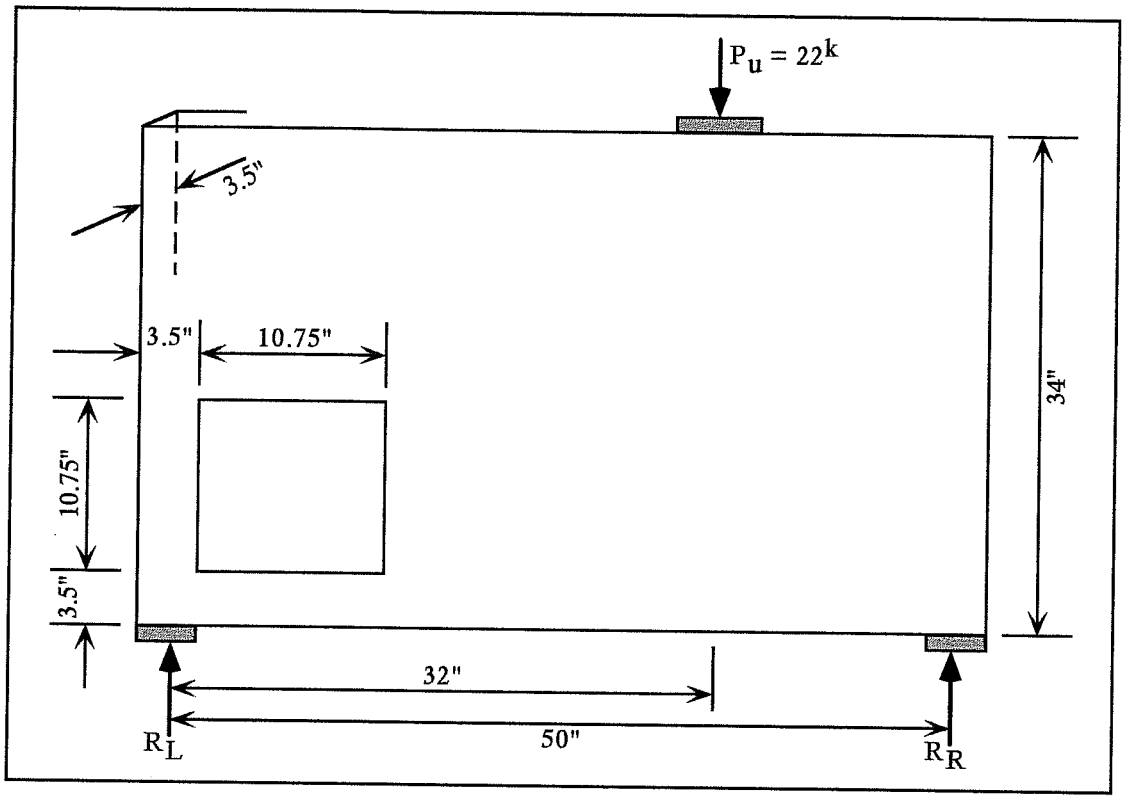

Figure 5-1 - Geometry of Deep Beam

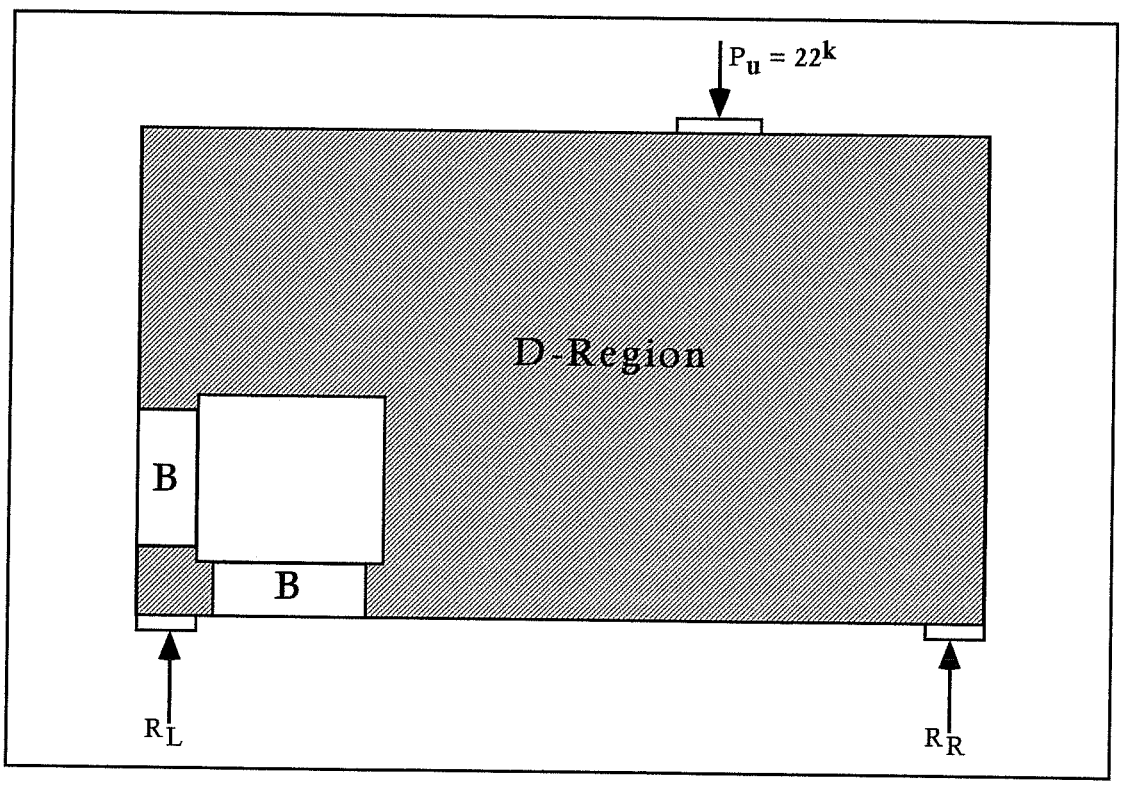

Figure 5-2 - B- and D-Regions of the Deep Beam

5.2. B- and D-Regions

The deep beams to be designed are essentially one large D-region. The strut-and-tie model technique will be employed to yield a design that accounts for all load paths in this D-region. However, as seen in Figure 5-2, there are two small B-regions located to the left and below the large opening that can be designed using traditional methods.

5.3. Design of B-Regions by Traditional Methods

The B-regions of the deep beam can be designed using the ACI Building Code 318-95. For the deep beam, as designed by Schlaich et al., no reinforcement was placed in the beam to the left of the hole. However, Schlaich et al. state, "The design engineer should provide further reinforcement, such as a mesh on either surface of the wall, nominal column reinforcement at the left of the hole, and stirrups below the hole."

Since the intent of this investigation is to test the strut-and-tie model, only extra reinforcement to the left of the hole is provided since that column is assumed to carry all of the load directed to the left support. Section 10.9.1 of ACI 318-95 specifies a minimum reinforcement for columns as 1 percent. This ratio is reduced to 0.5% to reflect that the section is much larger than required for the compression load (Bergmeister et al., 1993). Thus, $A_s = (0.005)(3.5\text{-in.})(3.5\text{-in.}) = 0.061\text{-in}^2$. From this, the column was designed with 4-3mm bars longitudinally and maximum tie spacing of 1-mm bars at 2.5-inches on center as specified by ACI 318-95 Section 7.10.5.2. No reinforcement is placed below the hole except for necessary anchorage of bars in specimens 1, 2, and 3. Specimen 4 has reinforcement below the hole to improve overall specimen integrity.

5.4. Specimen 1 - Design of D-Region

5.4.1. Strut-and-Tie Model

The strut-and-tie model used to design the first specimen is shown in Figure 5-3. This model is based on one of the strut-and-tie models designed by Schlaich et al. The load is distributed to the left and right support as dictated by statics and is carried by the strut-and-tie model between the load and support.

On the right side of the specimen, compatibility requirements cause the load to flow through stress fields that spread out between the nodes and fill available space (Bergmeister et al., 1993). This spreading results in transverse tensile stresses which must be considered in the design. Therefore, a bottle shaped strut-and-tie model is used with tensile ties at the top and bottom of the deep beam.

The left side of the strut-and-tie model was designed around the large opening. For the first specimen, the strut-and-tie model consists of horizontal, vertical, and 45-degree struts and ties except for the initial spreading of the point load. This allows for ease of reinforcement placement as will be discussed.

The right and left sides of the strut-and-tie model are connected with appropriate members and the forces of all members are calculated. Each strut and tie is classified by the magnitude of force it carries and whether it is compressive or tensile. These forces are given in Table 5-1. Thus, all forces in the deep beam strut-and-tie model are known and the reinforcement is designed to resist all tensile forces.

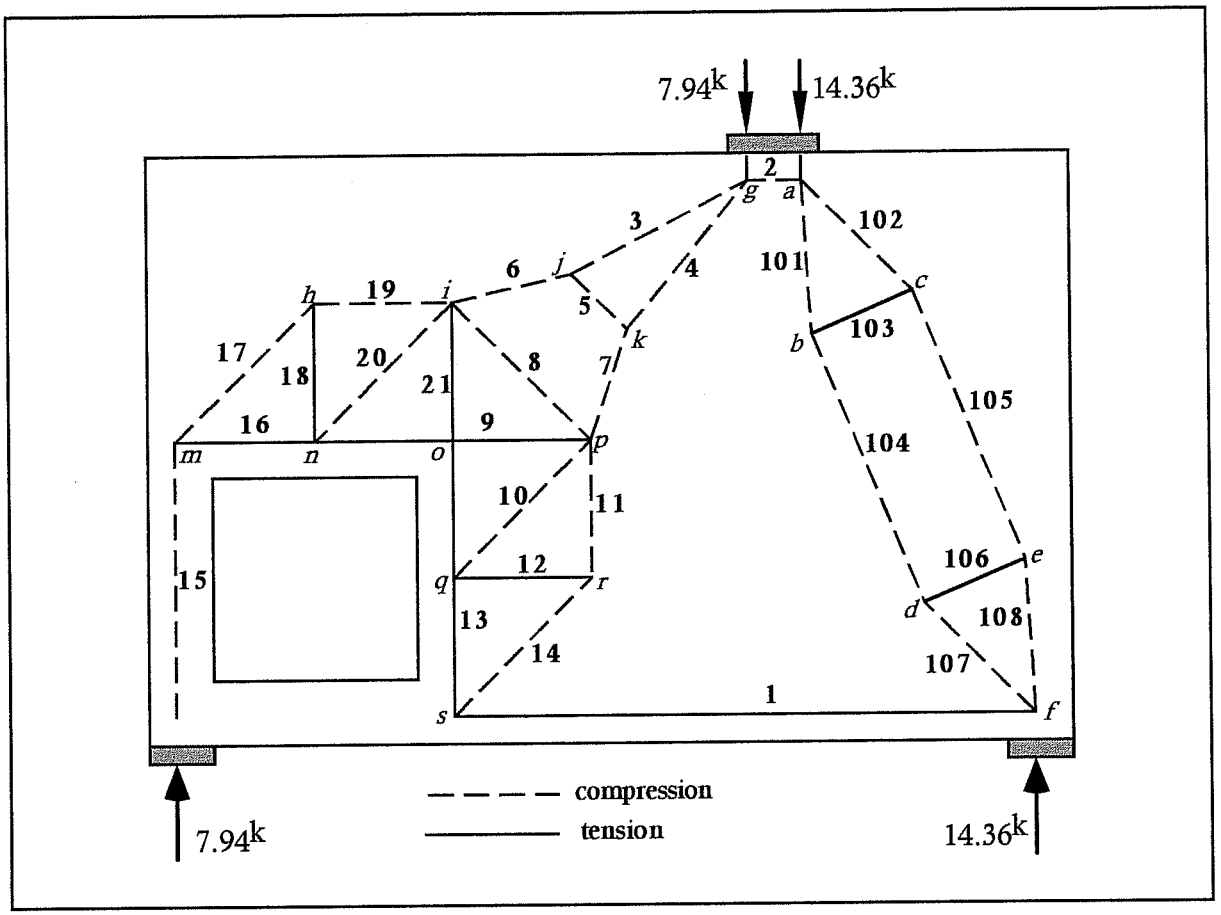

Figure 5-3 - Strut-and-Tie Model for Specimen 1

Table 5-1 - Geometry and Forces of Struts and Ties for Specimen 1

Member	Length (in)	Angle (deg)	Type	Force (kip)
1	35.66	0.0	T	7.82
2	2.50	0.0	C	7.82
3	11.55	35.1	C	5.87
4	11.55	51.0	C	5.87
5	3.17	45.0	C	2.09
6	7.51	17.4	C	6.34
7	7.51	72.6	C	6.34
8	10.41	45.0	C	13.90
9	14.34	0.0	T	15.88
10	10.14	45.0	C	11.23
11	7.17	90.0	C	7.94
12	7.17	0.0	T	7.94
13	7.17	90.0	T	7.94
14	10.14	45.0	C	11.23
15	14.34	90.0	C	7.94
16	7.17	0.0	T	7.94
17	10.14	45.0	C	11.23
18	7.17	90.0	T	7.94
19	7.17	0.0	C	7.94
20	10.14	45.0	C	11.23
21	14.34	90.0	T	15.88
101	8.21	83.0	C	8.79
102	8.21	41.0	C	8.79
103	5.71	28.0	T	3.15
104	19.78	62.0	C	8.13
105	19.78	62.0	C	8.13
106	5.71	28.0	T	3.15
107	8.21	40.0	C	8.79
108	8.21	82.0	C	8.79

5.4.2. Design of Reinforcement Bars

Once the forces are calculated for the strut-and-tie model, the reinforcement bars can be designed to resist all tensile forces that exist in the deep beam. The ties within the model dictate where the reinforcement bar will be placed. To determine how many bars need to be used along these tensile ties, the expected force is divided by the yield point of the reinforcement bar. This gives the area of steel needed. This area is divided by the bar area to give the number of bars needed for the tensile tie.

For the first specimen, there are three calculations that need to be done to design the seven tensile ties on the left side of the specimen. These calculations are given in Table 5-2. Note that for ties 1,9,13,16, and 21, 6-mm bars are used while 3-mm bars are used for ties 12 and 18. Notice that the amount of steel provided for ties 13 and 16 is much larger than required. This is because the bars that are used for ties 9 and 21 are extended to the edges of the specimen thus incorporating the lower force ties. The length of these bars is dictated by the strut-and-tie model and anchorage length requirements. Constructability is an additional consideration in determining bar placement.

Table 5-2 - Reinforcement Required for Specimen 1

Tension Tie	Force (kip)	As Required (in^2)	As Provided (in^2)	
1	7.82	0.095	3-6mm =	0.135
9	15.88	0.194	5-6mm =	0.225
12	7.94	0.093	5-3mm =	0.110
13	7.94	0.093	5-6mm =	0.225
16	7.94	0.093	5-6mm =	0.225
18	7.94	0.093	5-3mm =	0.110
21	15.88	0.194	5-6mm =	0.225

For the right side of the specimen, each model has the same strut-and-tie model as the load is transferred to the right support. A horizontal and vertical mesh is designed to cover the entire area on the right side of the specimen to resist the spreading of the compressive force. From the strut-and-tie model, tensile forces for ties 103 and 106 are known to be 3.15-kips. These forces are converted to their horizontal and vertical components using trigonometry which gives the horizontal and vertical tensile stresses. It was found, however, that ACI Code 318-95 Section 14.3 (Walls) governs the design by specifying a minimum ratio of reinforcement area to gross concrete area. For vertical steel, this ratio is 0.0012, and, for horizontal steel, the ratio is 0.0020. Thus, using 3-mm bar:

Vertical:

$$A_S = 0.0012(3.5in) = 0.0042\,{}^{in^2}\!/_{in} \Rightarrow 5.24\,{}^{in}\!/_{bar}$$

Horizontal:

$$A_S = 0.0020(3.5in) = 0.0070\,{}^{in^2}\!/_{in} \Rightarrow 3.14\,{}^{in}\!/_{bar}$$

Therefore, for the mesh on the right side of the specimen, 11 horizontal 3-mm bars 20-inches long spaced at 3-inches on center, and 5 vertical bars 30-inches long spaced at 5-inches on center were used. This mesh is used to resist all tensile forces that exist in the right side of the beam.

5.4.3. Anchorage Considerations

It is important to provide sufficient anchorage for the reinforcement bars. The anchorage length is considered to be extra length past the node where the struts and ties connect. For this purpose, the length of the tie plus necessary anchorage length dictates the final length of the reinforcement bars. Reference to members is shown in Figure 5-3. For example, for tie 21 and 13 the length of the tie is 21.5-inches. From Chapter 4, the anchorage

length for the 6-mm bar to develop the yield strength of the bar is 4.1-inches. Thus, for Specimen 1 there will be 5-6mm bars running along ties 13 and 21 for 26-inches. This provides anchorage for the bars past node i. For anchorage at node s, the anchorage length needed is not available, so the bars are looped around the horizontal steel. All other lengths are determined using the same logic. Figure 5-4 shows the reinforcement bar pattern ultimately used in construction of Specimen 1.

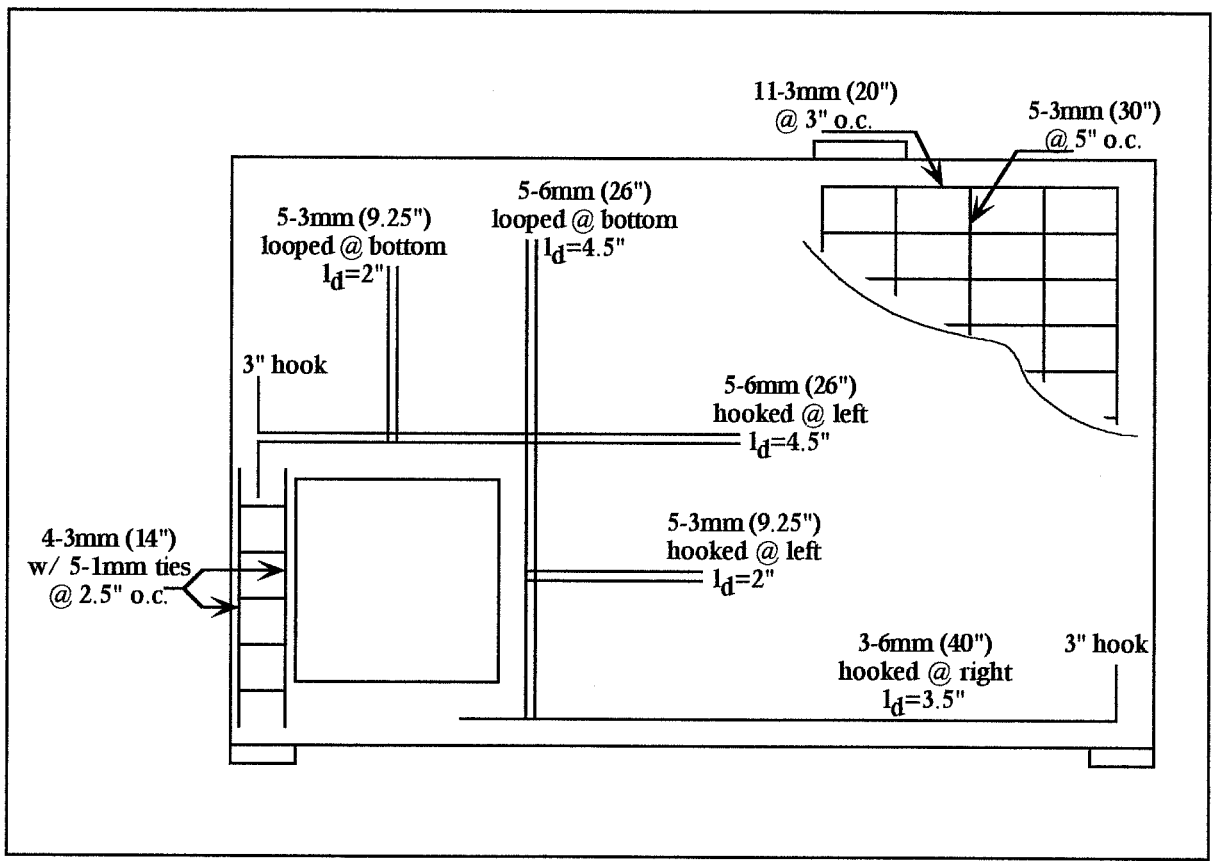

Figure 5-4 - Reinforcement Layout for Specimen 1

5.4.4. Node Checks

As mentioned previously, the nodes are of significant importance. There must be some assurance that the nodes can transfer the appropriate loads between the struts and ties.

For the deep beam strut-and-tie model, Schlaich et al. point out that the most heavily loaded node is near the right support at node f.

Node f (CCT): the geometry for this node is shown in Figure 5-5

$$w_1 = 3.5" \text{ and } w_T = 0.24"$$

$$w_2 = 3.5" \sin(62^\circ) + 0.24" \cos(62^\circ) = 3.20"$$

$$\sigma_{ca} = \frac{C_a}{w_2 b} = \frac{16.26^k}{3.20" \, x3.5"} = 1450psi$$

$$\leq \left[3200psi = 0.8(4000psi) = \nu_e f_c'\right] \text{ OK}$$

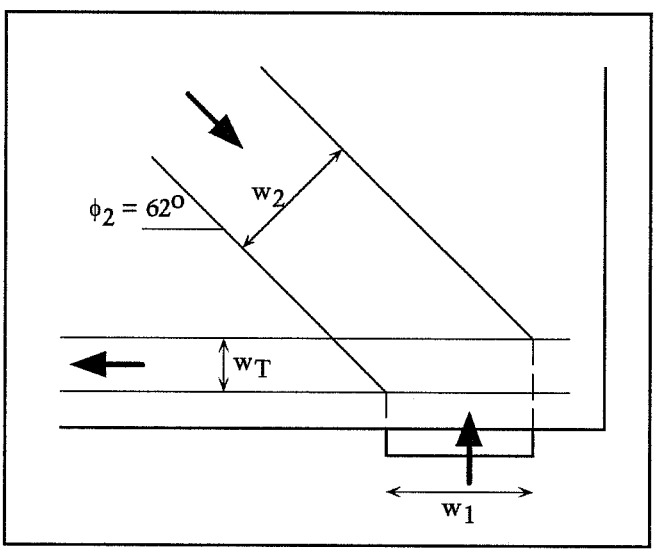

Figure 5-5 - Geometry of Node f

Thus, the stresses are low enough to consider this a safe solution.

5.5. Specimen 2 - Design of D-Region

5.5.1. Strut-and-Tie Model

The strut-and-tie model used to design the second specimen is shown in Figure 5-6. This model is based on the other strut-and-tie model designed by Schlaich et al. As with the

first specimen, this strut-and-tie model carries the entire load and distributes portions of that load to the left and right support.

The right side of the specimen is the same as for Specimen 1. Thus, it is modeled and designed as before. The left side of the strut-and-tie model for Specimen 2 is a much simpler model than Specimen 1. There are three compression struts and one tensile tie carrying the load. The tension tie is oriented at a 45-degree angle and provides the vertical reaction from compression strut 6. The forces for each member are calculated and given in Table 5-3. Knowing the forces in the model, the reinforcement is designed.

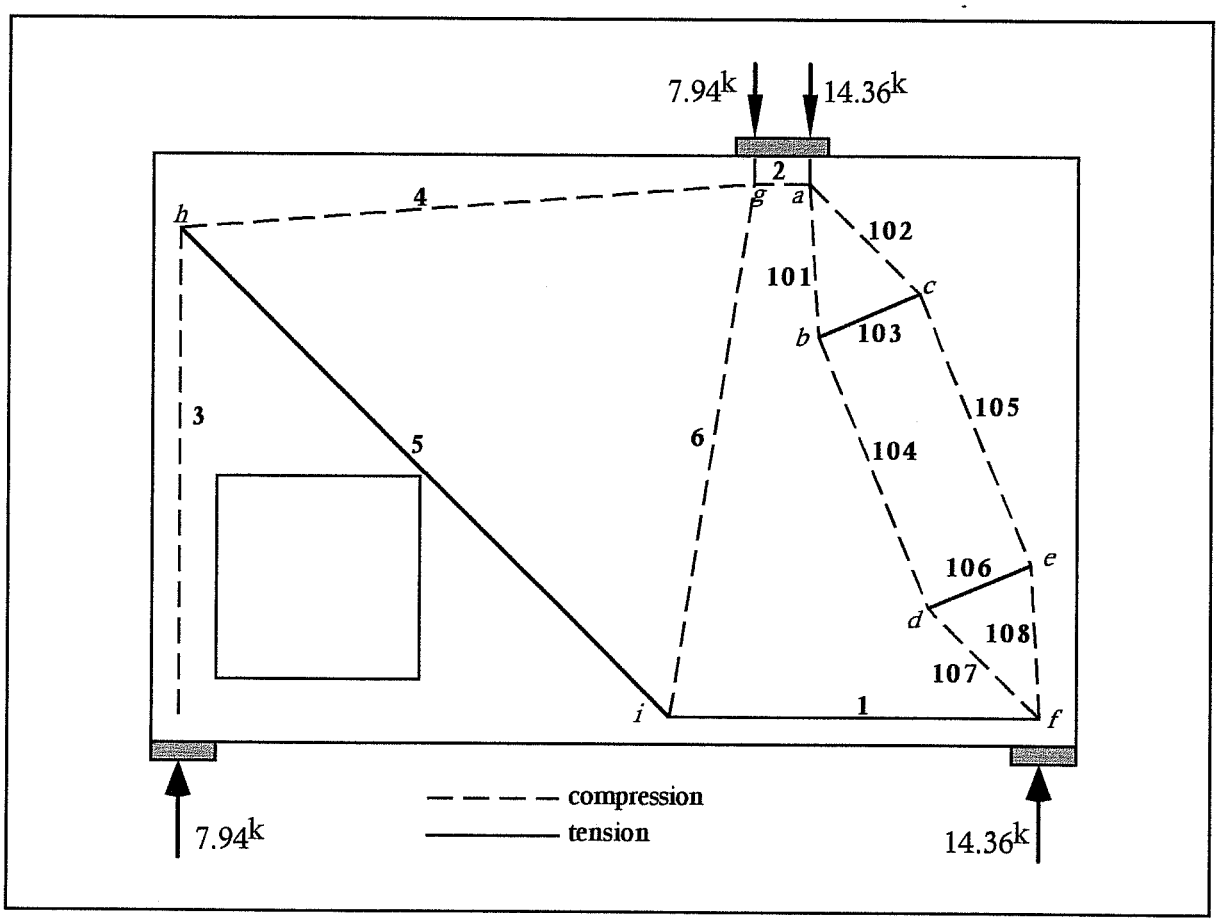

Figure 5-6 - Strut-and-Tie Model for Specimen 2

Table 5-3 - Geometry and Forces of Struts and Ties for Specimen 2

Member	Length (in)	Angle (deg)	Type	Force (kip)
1	23.95	0.0	T	7.82
2	2.50	0.0	C	7.82
3	26.05	90.0	C	7.94
4	31.25	8.0	C	7.03
5	36.84	45.0	T	9.85
6	30.79	80.8	C	7.05
101	8.21	83.0	C	8.79
102	8.21	41.0	C	8.79
103	5.71	28.0	T	3.15
104	19.78	62.0	C	8.13
105	19.78	62.0	C	8.13
106	5.71	28.0	T	3.15
107	8.21	40.0	C	8.79
108	8.21	82.0	C	8.79

5.5.2. Design of Reinforcement Bars

The forces given in Table 5-3 are used to design the necessary reinforcement bars. The bars are used to carry all tension loads within the strut-and-tie model. The design is done in the same manner as Specimen 1. For Specimen 2, there are only two tensile ties on the left side of the model. The calculations for member 1 and 5 are given in Table 5-4. Again, anchorage length and the length of the ties dictate the length of the reinforcement bars. The right side of the specimen is designed exactly as Specimen 1.

Table 5-4 - Reinforcement Required for Specimen 2

Tension Tie	Force (kip)	As Required (in^2)	As Provided (in^2)
1	7.82	0.095	3-6mm = 0.135
5	9.85	0.120	3-6mm = 0.135

5.5.3. Anchorage Considerations

The anchorage of the bars running along members 1 and 5 is provided by making these bars continuous. There are three bars that continuously run from node f to node i to node h. At each end of these bars, there is not sufficient room to provide anchorage for straight bars so each end has a 3-inch 90-degree hook. This provides sufficient anchorage for the ends of the bars. The reinforcement for Specimen 2 is shown in Figure 5-7.

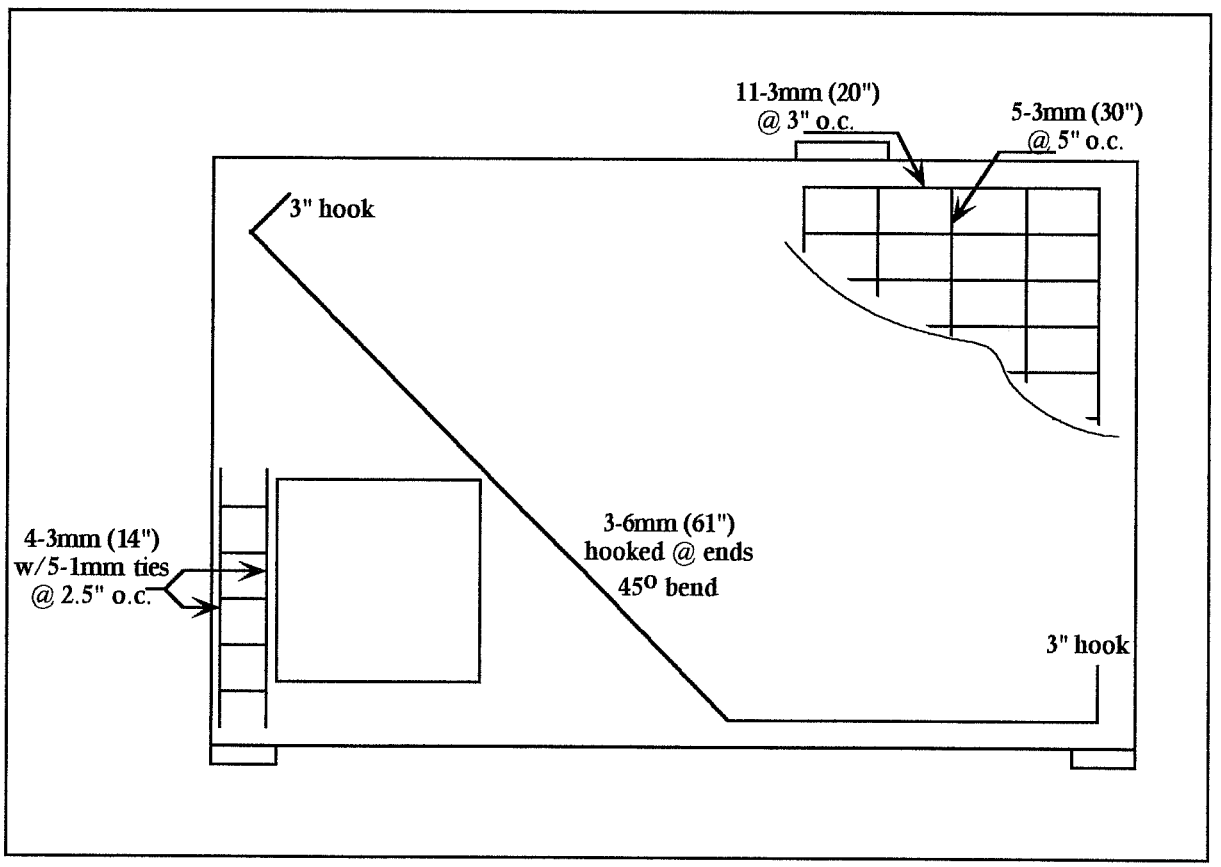

Figure 5-7 - Reinforcement Layout for Specimen 2

5.6. Specimen 3 - Design of D-Region

5.6.1. Strut-and-Tie Model

The strut-and-tie model used to design the third specimen is shown in Figure 5-8. This specimen is based on the same design performed by Schlaich et al. The right side of the strut-and-tie model is the same as the previous models. The left side consists of a combination of the two previous models. Each model is assumed to carry half of the applied load. The forces for the members are calculated and given in Table 5-5.

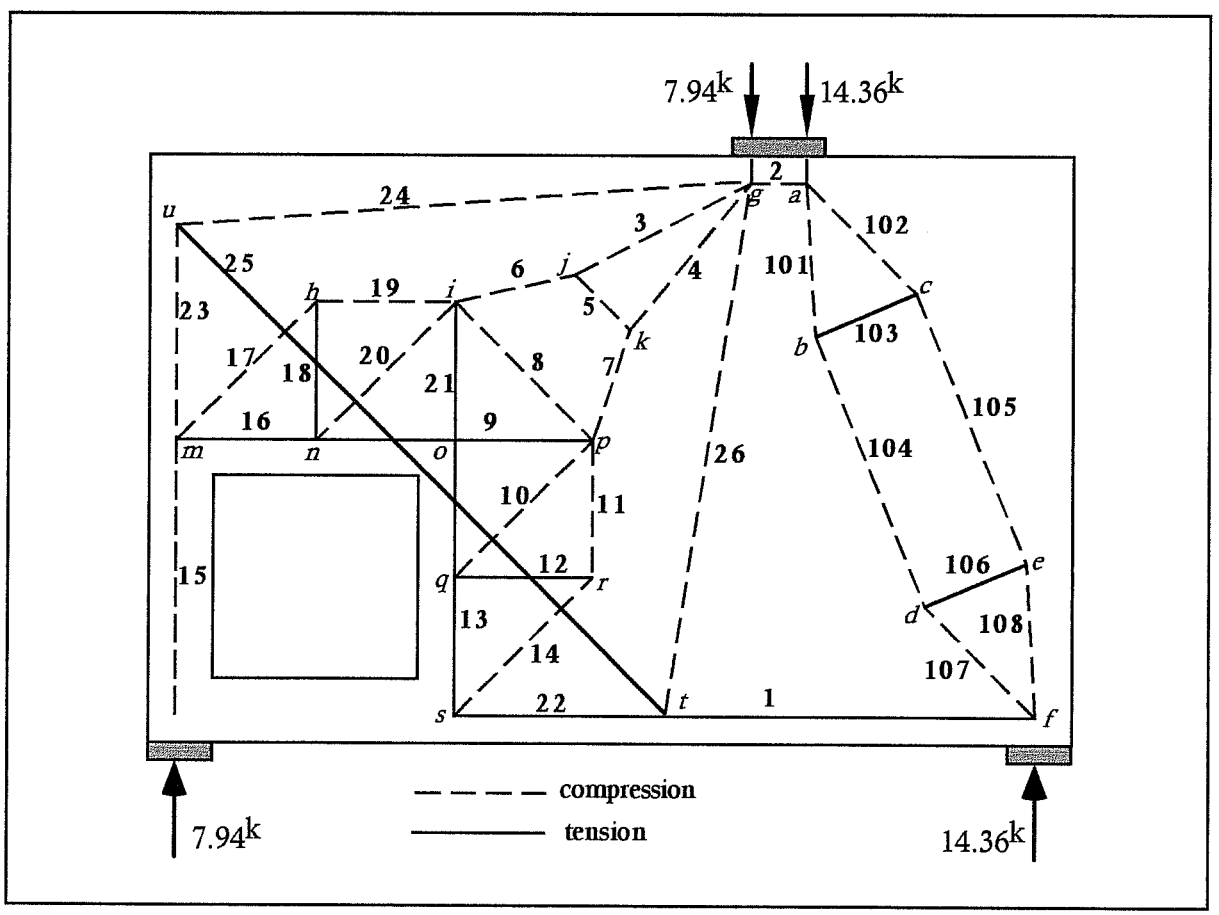

Figure 5-8 - Strut-and-Tie Model for Specimen 3

Table 5-5 - Geometry and Forces of Struts and Ties for Specimen 3

Member	Length (in)	Angle (deg)	Type	Force (kip)
1	35.66	0.0	T	7.82
2	2.50	0.0	C	7.82
3	11.55	35.1	C	2.94
4	11.55	51.0	C	2.94
5	3.17	45.0	C	1.05
6	7.51	17.4	C	3.17
7	7.51	72.6	C	3.17
8	10.41	45.0	C	6.95
9	14.34	0.0	T	7.94
10	10.14	45.0	C	5.62
11	7.17	90.0	C	3.97
12	7.17	0.0	T	3.97
13	7.17	90.0	T	3.97
14	10.14	45.0	C	5.62
15	14.34	90.0	C	7.94
16	7.17	0.0	T	3.97
17	10.14	45.0	C	5.62
18	7.17	90.0	T	3.97
19	7.17	0.0	C	3.97
20	10.14	45.0	C	5.62
21	14.34	90.0	T	7.94
22	11.71	0.0	T	3.97
23	36.05	90.0	C	3.97
24	31.25	8.0	C	3.52
25	36.84	45.0	T	4.93
26	30.79	80.8	C	3.53
101	8.21	83.0	C	8.79
102	8.21	41.0	C	8.79
103	5.71	28.0	T	3.15
104	19.78	62.0	C	8.13
105	19.78	62.0	C	8.13
106	5.71	28.0	T	3.15
107	8.21	40.0	C	8.79

5.5.2. Design of Reinforcement Bars

The forces given in Table 5-5 are used to design the necessary reinforcement bars. Reinforcement bars will carry all tension loads within the strut-and-tie model. The required reinforcement is calculated and given in Table 5-6.

Table 5-6 - Reinforcement Required for Specimen 3

Tension Tie	Force (kip)	As Required (in^2)	As Provided (in^2)	
1	7.82	0.095	3-6mm =	0.135
9	7.94	0.097	3-6mm =	0.135
12	3.97	0.046	3-3mm =	0.066
13	3.97	0.046	3-6mm =	0.135
16	3.97	0.046	3-6mm =	0.135
18	3.97	0.046	3-3mm =	0.066
21	7.94	0.194	3-6mm =	0.135
22	3.97	0.048	1-6mm =	0.045
25	4.93	0.060	2-6mm =	0.090

5.6.3. Anchorage Considerations

The anchorage for each of the bars is taken care of in the same manner as explained for Specimen 1 and Specimen 2. The reinforcement pattern for Specimen 3 is shown in Figure 5-9.

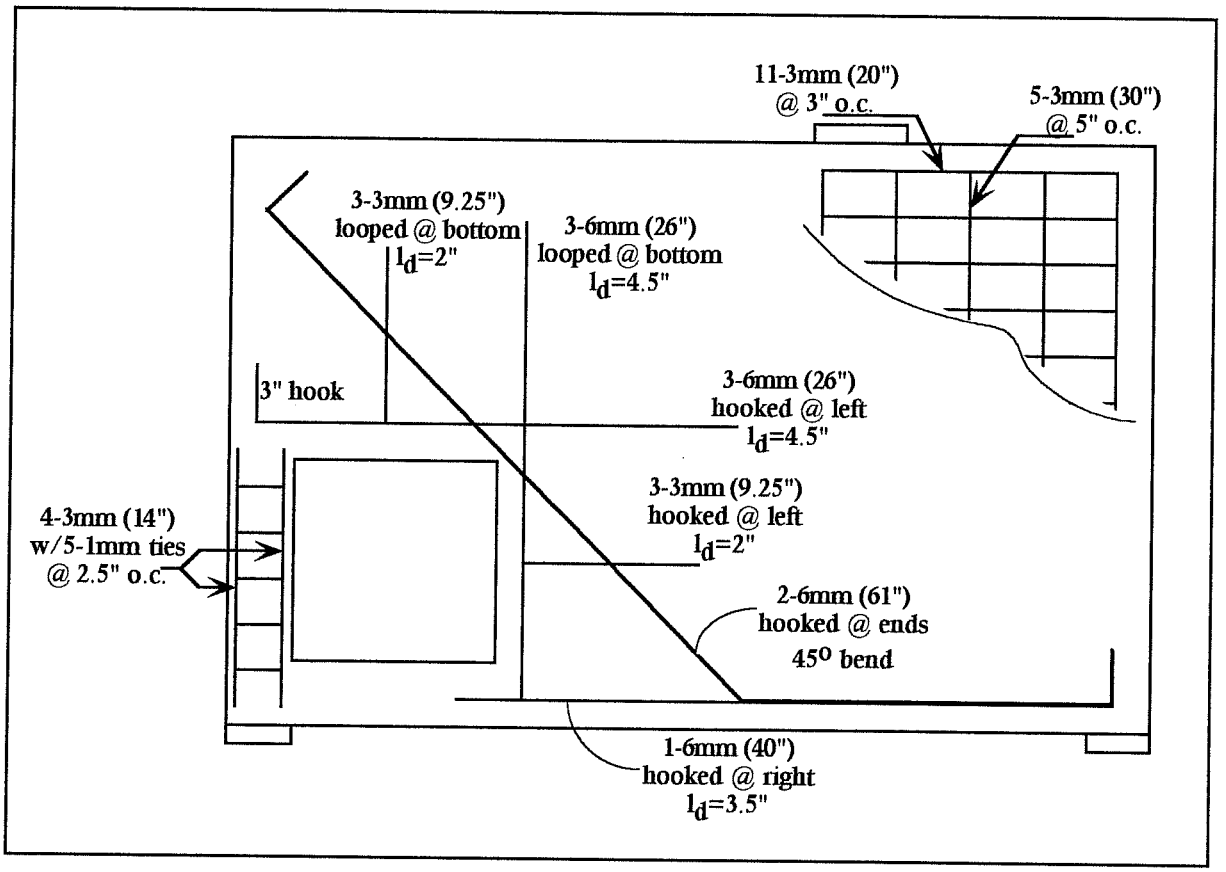

Figure 5-9 - Reinforcement Layout for Specimen 3

5.7. Specimen 4 - Design of D-Region

5.7.1. Strut-and-Tie Model

The strut-and-tie model used to design the fourth specimen is shown in Figure 5-10. This model is a variation on the model designed by Schlaich et al. The three previous specimens were designed using strut-and-tie models which assume that all force will be transferred through the column on the left side of the hole. However, if this deep beam had no hole in it, beam theory would indicate that the bottom face of the beam would experience tensile forces. Therefore, the fourth strut-and-tie model is modified to create a tensile force in the strut-and-tie model below the large opening. Other than this additional force, the model is

the same as that in Specimen 3, and is designed in a similar fashion. The forces for each member are calculated and given in Table 5-7. Knowing these forces, the reinforcement is designed.

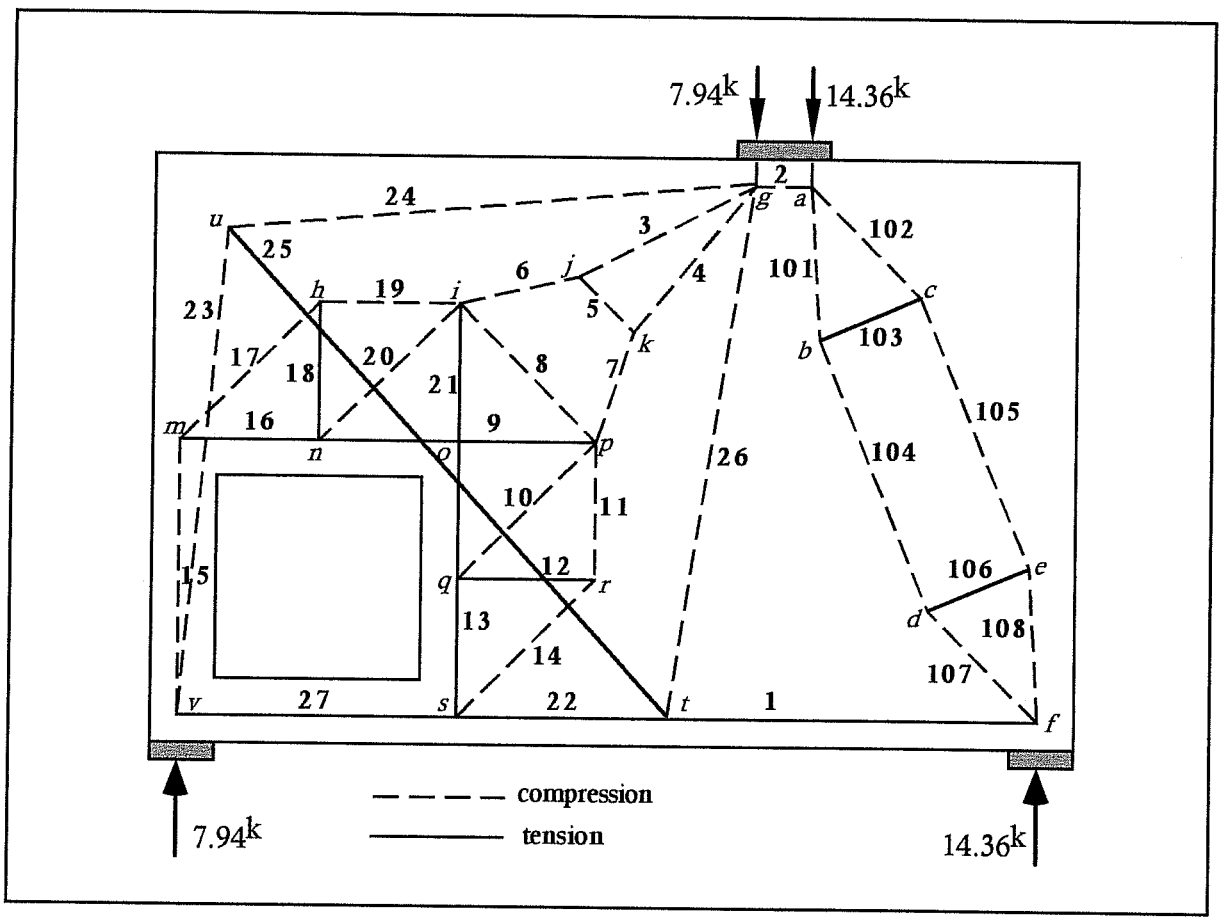

Figure 5-10 - Strut-and-Tie Model for Specimen 4

Table 5-7 - Geometry and Forces of Struts and Ties for Specimen 4

Member	Length (in)	Angle (deg)	Type	Force (kip)
1	35.66	0.0	T	7.82
2	2.50	0.0	C	7.82
3	11.55	35.1	C	2.94
4	11.55	51.0	C	2.94
5	3.17	45.0	C	1.05
6	7.51	17.4	C	3.17
7	7.51	72.6	C	3.17
8	10.41	45.0	C	6.95
9	14.34	0.0	T	7.94
10	10.14	45.0	C	5.62
11	7.17	90.0	C	3.97
12	7.17	0.0	T	3.97
13	7.17	90.0	T	3.97
14	10.14	45.0	C	5.62
15	14.34	90.0	C	7.94
16	7.17	0.0	T	3.97
17	10.14	45.0	C	5.62
18	7.17	90.0	T	3.97
19	7.17	0.0	C	3.97
20	10.14	45.0	C	5.62
21	14.34	90.0	T	7.94
22	11.71	0.0	T	3.97
23	26.17	85.0	C	3.97
24	28.75	8.0	C	3.52
25	35.13	52.0	T	4.93
26	30.79	80.8	C	3.53
27	14.34	0.0	T	0.35
101	8.21	83.0	C	8.79
102	8.21	41.0	C	8.79
103	5.71	28.0	T	3.15
104	19.78	62.0	C	8.13
105	19.78	62.0	C	8.13
106	5.71	28.0	T	3.15
107	8.21	40.0	C	8.79
108	8.21	82.0	C	8.79

5.7.2. Design of Reinforcement Bars

The forces given in Table 5-7 are used to design the necessary reinforcement bars. The design is done in the same manner as that for Specimen 3, and the layout of bars is the same as that for Specimen 3 except for the additional bars below the hole. The reinforcement used is give in Table 5-8.

Table 5-8 - Reinforcement Required for Specimen 4

Tension Tie	Force (kip)	As Required (in^2)	As Provided (in^2)	
1	7.82	0.095	3-6mm =	0.135
9	7.94	0.097	3-6mm =	0.135
12	3.97	0.046	3-3mm =	0.066
13	3.97	0.046	3-6mm =	0.135
16	3.97	0.046	3-6mm =	0.135
18	3.97	0.046	3-3mm =	0.066
21	7.94	0.194	3-6mm =	0.135
22	3.97	0.048	1-6mm =	0.045
25	4.93	0.060	2-6mm =	0.090
27	0.35	0.004	2-6mm =	0.090

5.7.3. Anchorage Considerations

The same concern exists for the anchorage of bars in Specimen 4 as it does for all other specimens. The anchorage is the same as Specimen 3 with the exception that the two bars that run the length of the beam on the bottom are hooked at each end. The reinforcement for the specimen is shown in Figure 5-11.

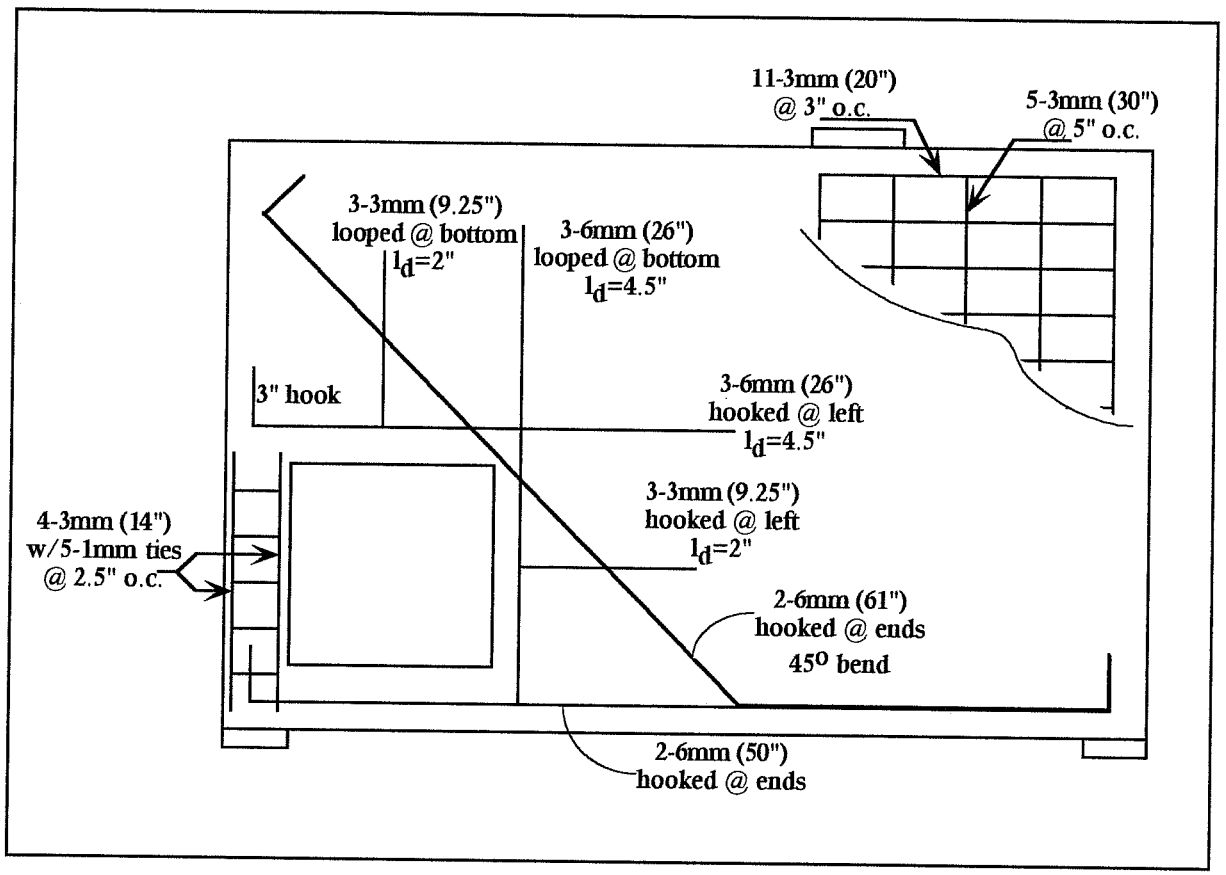

Figure 5-11 - Reinforcement Layout for Specimen 4

5.8. Conclusion

In this chapter, all analysis and design of the deep beam specimens has been presented. The four specimens were based on strut-and-tie models used singly and in combination. The four strut-and-tie models have been developed and analyzed to determine forces that each model will be required to resist. Reinforcement bars have been designed based on these forces and anywhere in the strut-and-tie models where there is a tensile force, steel bars are placed. The layout and placement of the reinforcement bars is shown for each model. The figures in this chapter illustrate the layout of the beams as they were constructed. The specimens were cast and then tested.

CHAPTER 6

EXPERIMENTAL PROCEDURES

6.1. Fabrication

A total of four deep beams were fabricated and tested. Each beam was used to test the design of one of the strut-and-tie models presented in Chapter 5. The beams were cast using the concrete mix described in Chapter 3. Form-work was constructed, the reinforcement was arranged and tied in the forms, and the beams were cast and cured. In addition to the deep beams, a number of cylinders were prepared for each beam to monitor the concrete strength.

6.1.1. Form-work

Forms were constructed for each of the four specimens. The forms were made of ¾-inch plywood and lumber to frame the beam. Styrofoam was used to frame the large opening. A coat of form-release agent was applied to the entire form prior to casting.

6.1.2. Reinforcement Cage

The reinforcement cages and form-work for each of the four specimens are shown in Figure 6-1. These cages follow designs presented in Chapter 5. The column reinforcement steel to the left of the large opening and the reinforcing mesh on the right side are the same for all specimens. The reinforcement cages were made using 3-mm and 6-mm bars as specified in Chapter 5. To assure proper positioning, the reinforcement bars were tied together and held in position using small wooden blocks.

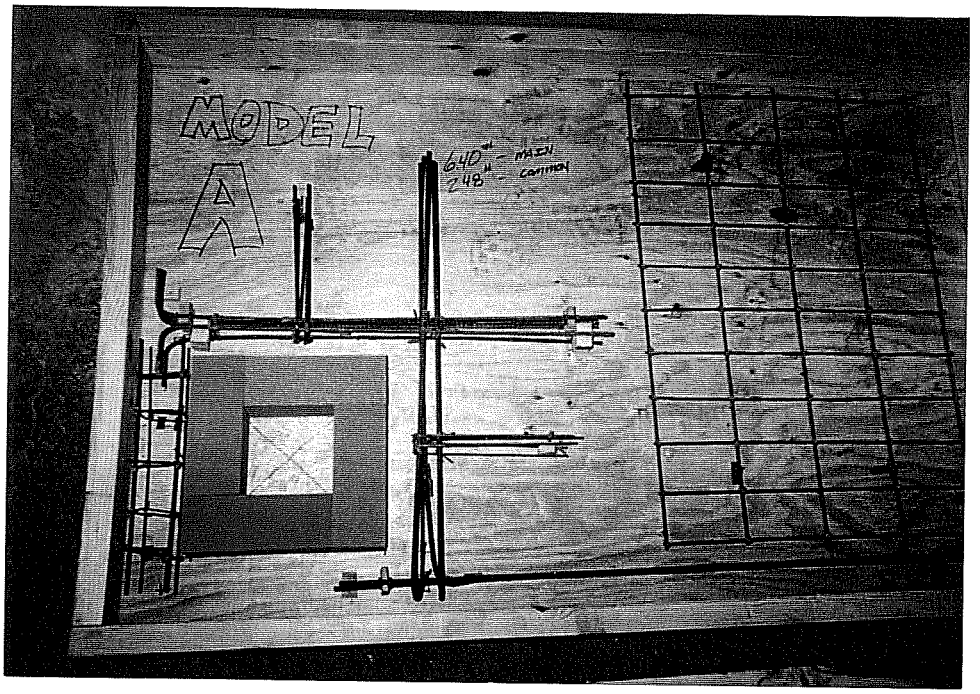

A.) Specimen 1

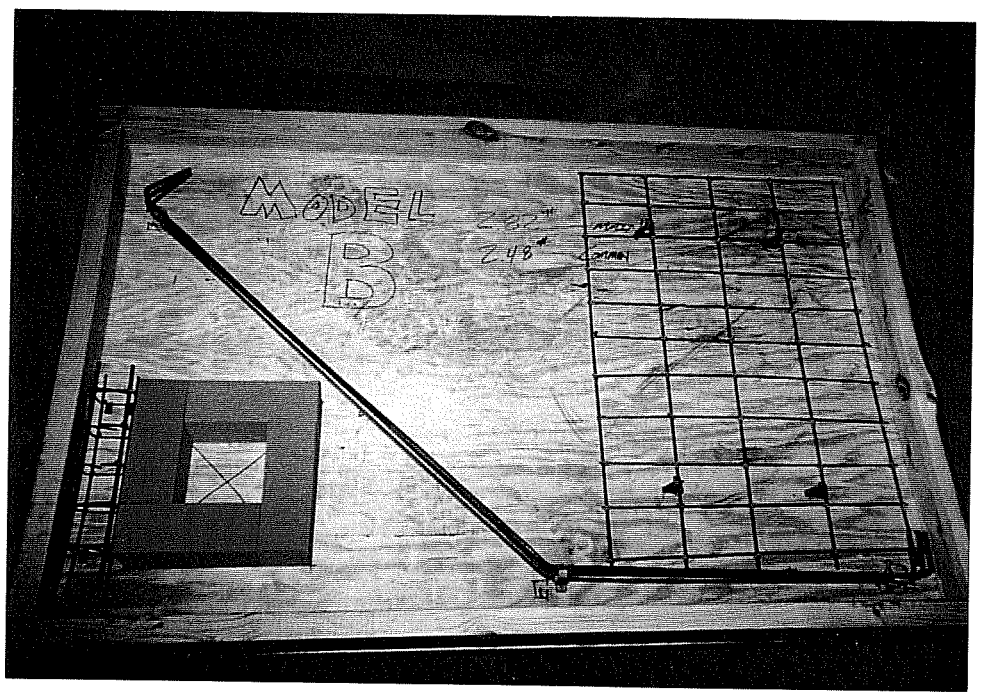

B.) Specimen 2

Figure 6-1 - Deep Beam Reinforcement and Form-work

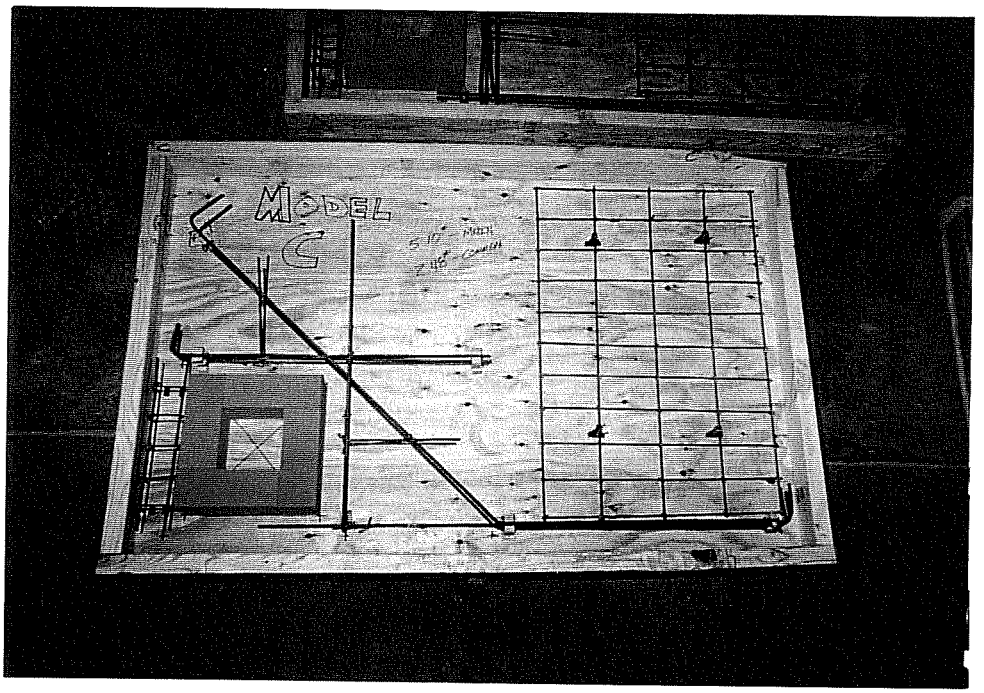

C.) Specimen 3

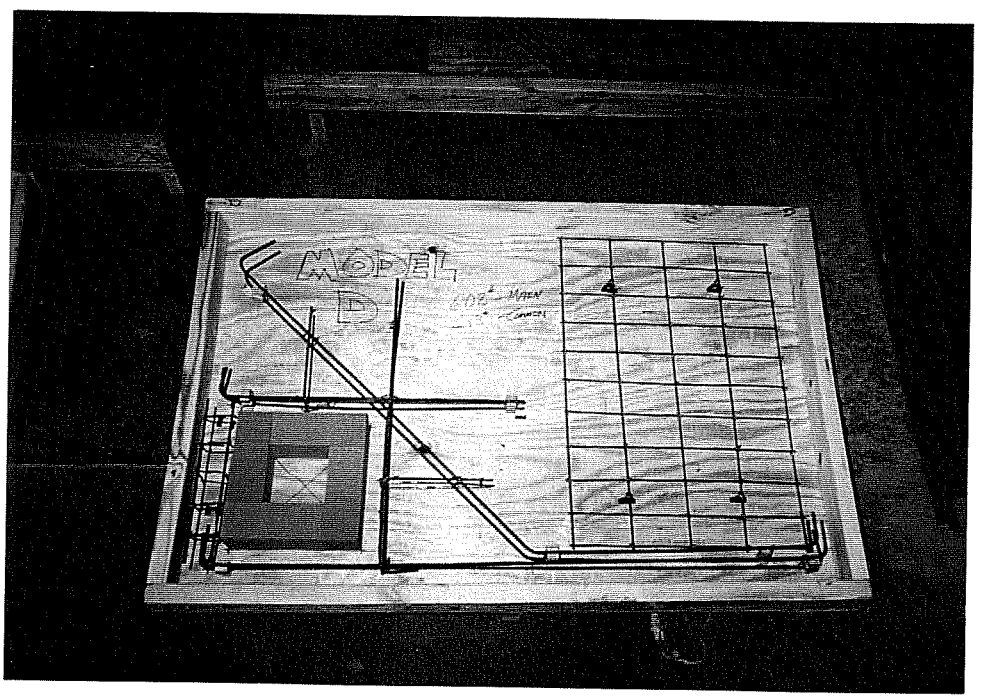

D.) Specimen 4

Figure 6-1 - Deep Beam Reinforcement and Form-work

6.1.3. Casting and Curing

The concrete was mixed using the ingredients discussed in Chapter 3. The pre-mixed sack concrete was mixed with water and the superplasticizer using an electric concrete mixer. Concrete was placed in the forms by hand and rodded into place. Concrete cylinders were cast from the mix used for each beam. The specimens were allowed to set, and then covered with damp burlap and plastic sheeting to maintain a constant moisture condition. The specimens were cured in the laboratory at a temperature between 75°F and 90°F. After 7 days, the forms were removed, and the specimens were again covered with wet burlap and plastic sheeting until day 28, when they were tested.

6.2. Testing Procedures

The four specimens were tested using a 600-kip universal test machine at the Ferguson Structural Engineering Laboratory at The University of Texas at Austin. The test machine is a displacement based machine. A point load was applied by the test machine to the top of the specimen which was supported on two concrete blocks. A steel frame was placed around the bottom of the specimen to prevent any out-of-plane movement of the specimen. This steel frame did not touch the specimen at any time. Rubber pads were placed under the two supports and under the point load. The test setup is shown in Figure 6-2.

Initially, the specimen was loaded in 2.5-kip increments with dial gage readings being taken at each step. Using a marker, crack lengths were highlighted and loads noted at each step. At 18-kips, the loading increment was reduced to 1-kip increments. This continued past the design load of 22-kips to failure of the specimen. Failure was determined by continued deflection of the beam and a decrease in the load carrying capacity of the beam.

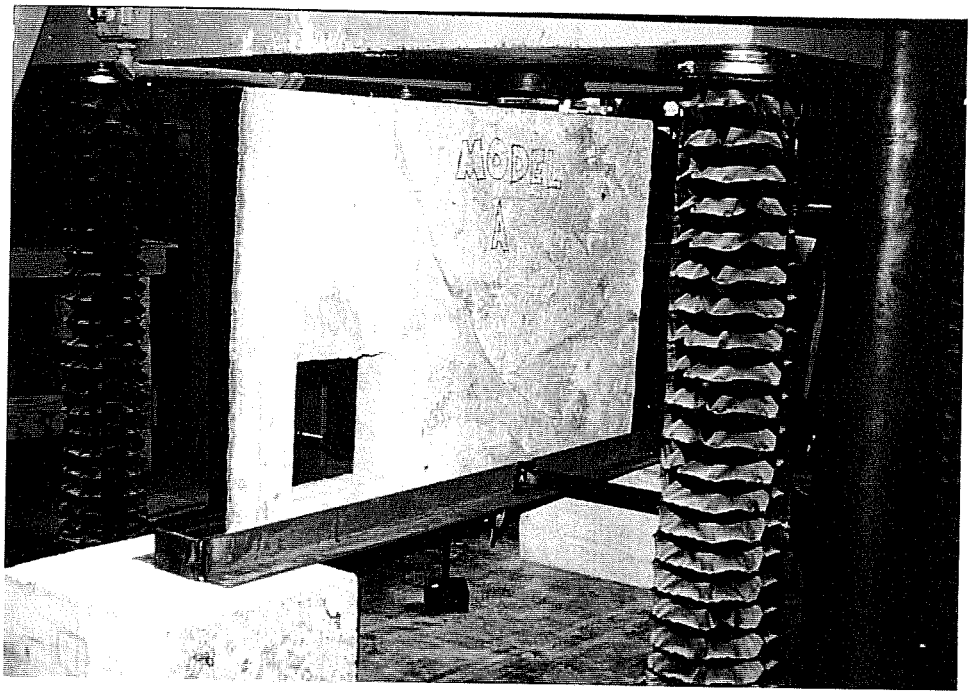

Figure 6-2 - Test Setup

6.2.1. Instrumentation

To record deflection of the beam, a dial gage was placed under the beam, directly below the point load. From this dial gage reading, accurate to 0.001-inch, a load-deflection curve was plotted. The load applied to the specimen was measured by the test machine.

6.2.2. Testing Problems and Solutions

For the test, it was extremely important to line the specimen directly below the point load. If the point load was not applied directly along the centroidal axis of the beam, bending of the tall, narrow specimen would occur. For the first test, it was found that the rubber pad beneath the point load was too small and bearing failure occurred. This was corrected by using a larger bearing pad to reduce the concentration of the load. The first specimen that experienced the bearing failure was repaired using a two part epoxy resin normally used for

reinforced concrete bridge repair. This reconstructed the damaged area and the test was repeated with the larger bearing pad.

CHAPTER 7

TEST RESULTS

7.1. Introduction

Test results were heartening for each specimen. All specimens carried more than the factored design load of 22-kips. This chapter will present all data recorded from the tests and failure crack patterns of the four specimens. Deflections were recorded using a dial gage, and a plot of load versus deflection was made to compare the behavior of the specimens. Deflections were not recorded for the entire test. After significant cracking had occurred, the dial gage was removed to protect the instrument. In the following sections, the specimen performance and cracking patterns are given.

7.2. Specimen 1

7.2.1. Specimen Performance and Results

Specimen 1 contained only horizontal and vertical reinforcement. The performance of this specimen was good. The specimen contained 8.9-lbs. of steel reinforcement and carried an ultimate load of 31-kips. The specimen reached its ultimate load during the second loading attempt.

Two tests were performed on the first specimen. First, the specimen was loaded with a 3.5-inch square rubber loading pad on top of the specimen. The first observable crack at 21-kips ran vertically with its origin at the lower left corner of the large hole. The loading continued until 24-kips when there was a bearing failure below the loading pad. Since this failure did not test the strut-and-tie model, except to say that it carried the required load, the

bearing failure was repaired using a two part epoxy and the beam was tested again on the following day.

After the specimen was repaired, a larger bearing pad, 7.5-inches long, was used to reduce the bearing stress under the load. This larger bearing pad was used for all subsequent tests. The second test was more productive in evaluating the strut-and-tie model of the first specimen. The beam was already cracked at the lower left corner of the hole and the next crack was observed radiating from the upper right corner at a 45-degree angle. This second crack occurred at a load of 17-kips.

At a load of 25-kips, the beginning of the ultimate failure crack formed. This crack, which ran from the upper left corner of the hole, over the top of the vertical bars, and to the load, was produced by shear. Other cracks formed but ultimately this specimen failed in shear at 31-kips. The final cracking pattern can be seen in Figure 7-1.

The concrete below the hole eventually cracked through at both ends and fell away. Although not desirable from a serviceability viewpoint, this was acceptable because the entire force from the load was transferred safely through the column on the left side of the hole. The column remained undamaged throughout the test. The right side of the specimen performed well also. No visible cracks were seen, although a vertical crack formed directly to the left of the steel reinforcement mesh that covered the right side.

Figure 7-5 shows the load-deflection curve in comparison to the other specimens. For this first specimen, the curve can be seen to be linear until about 17-kips when cracking occurs. Again, the load-deflection curve does not extend until failure.

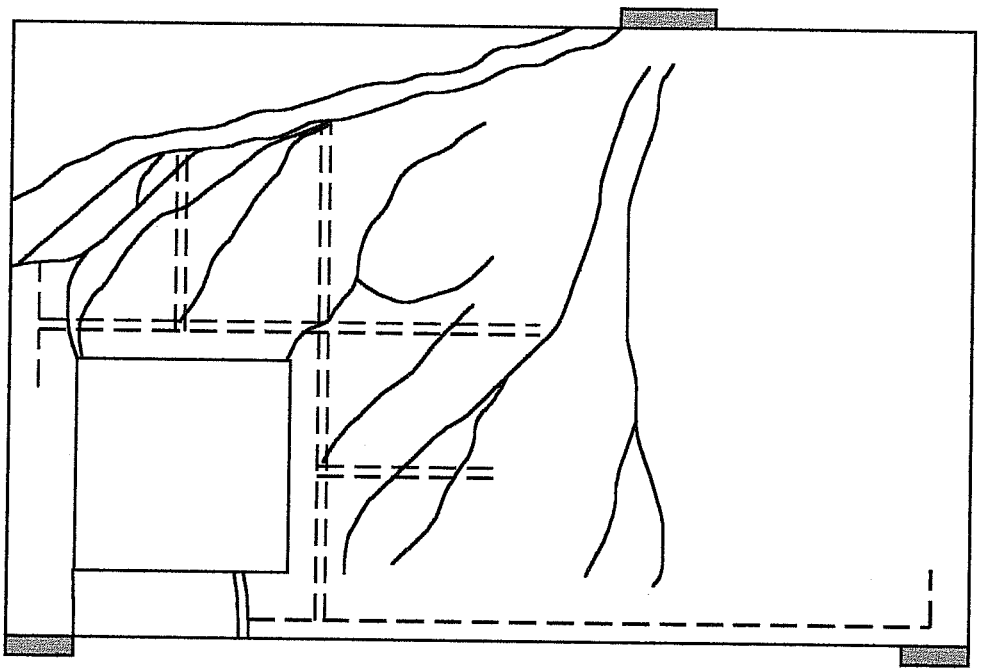

A.) Cracking Pattern

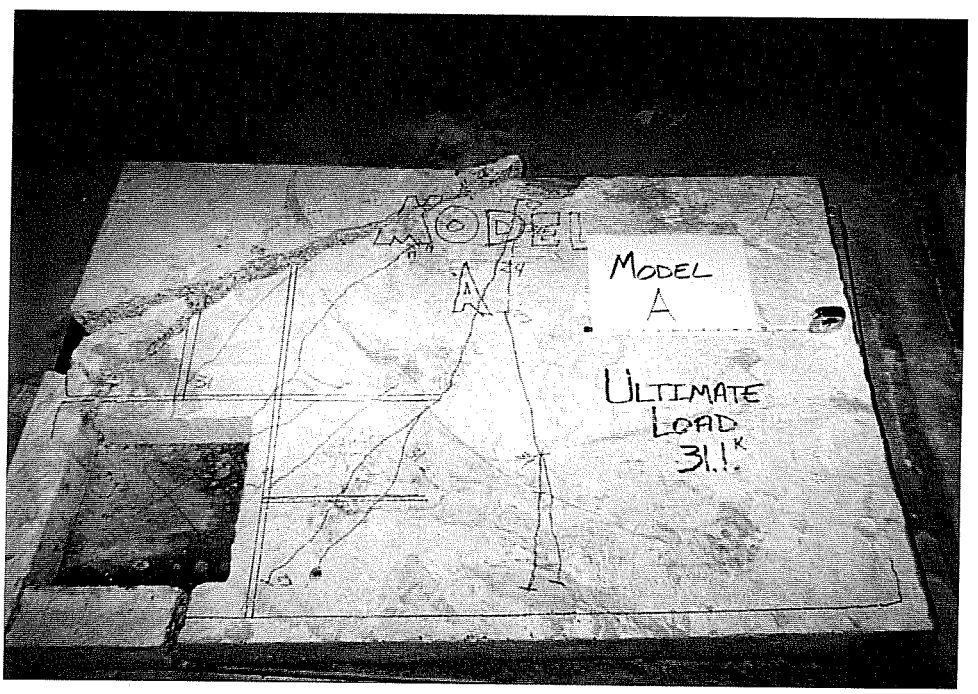

B.) Photograph of Cracking Pattern

Figure 7-1 - Cracking Pattern for Specimen 1

7.3. Specimen 2

7.2.1. Specimen Performance and Results

Specimen 2 had the simplest pattern of reinforcement. It contained 5.3-lbs. of steel and held a load of 33-kips. This loading occurred while using the larger bearing pad. The first cracks formed at the lower left corner of the opening as a vertical flexural crack at 18-kips. Also at 18-kips, a crack formed at a 45-degree angle radiating from the upper right corner of the opening. This caused a reduced stiffness of the specimen which can be seen on the load-deflection curve in Figure 7-5. Further cracks formed in a fan shape pattern from the loading point to the bars as the steel bars began to stretch. The concrete to the right of the hole and below the steel bars essentially cracked and fell out of the specimen as the specimen reached 30-kips. The beam ultimately failed at 33-kips with the steel reinforcement totally exposed along the length of greatest strain.

As in Specimen 1, the concrete below the hole cracked at both ends and fell away. The entire load was carried through the column on the left of the hole and no physical damage occurred to the column. The complete cracking pattern is shown in Figure 7-2. The specimen ultimately failed along a crack parallel and perpendicular to the reinforcement bar. Its stiffness was further reduced at about 23-kips.

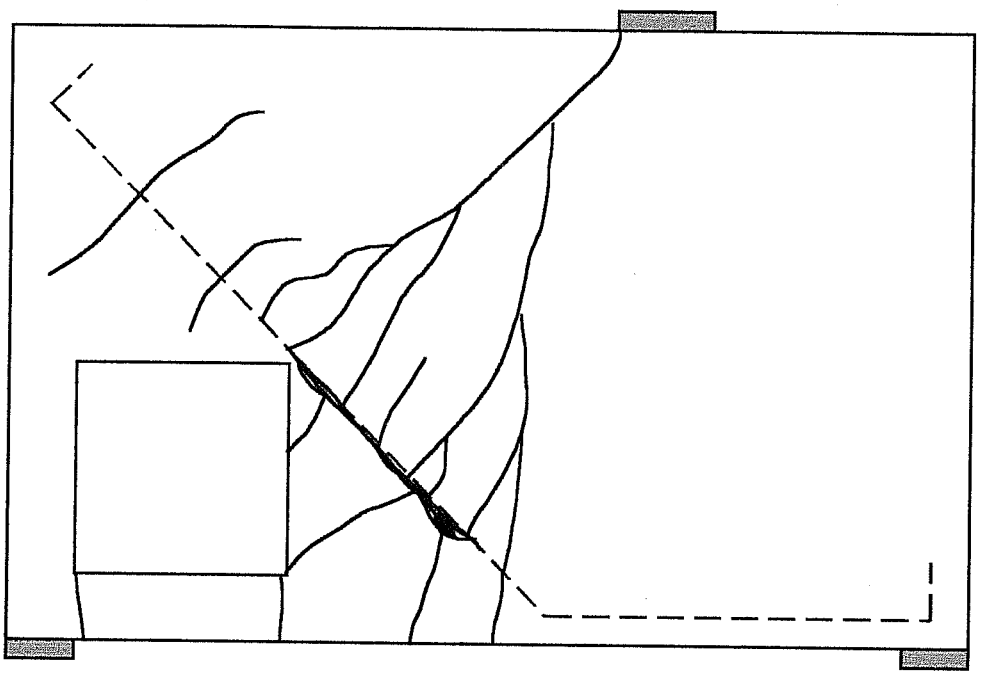

A.) Cracking Pattern

B.) Photograph of Cracking Pattern

Figure 7-2 - Cracking Pattern for Specimen 2

7.4. Specimen 3

7.4.1. Specimen Performance and Results

Specimen 3 used the reinforcement pattern and strut-and-tie model designed by Schlaich et al. It contained 7.6-lbs. of steel and withstood 41-kips of load. Characteristically, the first crack formed at the lower left corner of the hole at 18-kips. At 22-kips a small crack formed at 45-degrees from the upper right corner of the opening. Similar to Specimen 1, cracks ran from the column to the load, over the top of the vertical reinforcing bars. At about 28-kips, these cracks stopped growing and a major crack formed from the load along the left of the right side mesh and directly to the bend in the longitudinal bars. The crack pattern can be seen in Figure 7-3.

At 31-kips, the crack from the load to the bend in the longitudinal bars had become excessive, and at node t (see Figure 7-3), the concrete failed in compression and bulged out of the specimen. Cracks also formed at the upper left part of the specimen where the bent reinforcement bar terminated. Ultimately, the specimen was being held only by the reinforcement bar curving throughout the entire specimen. Around 40-kips, the column started to crumble and the specimen carried no further load. The specimen essentially split into two pieces.

From Figure 7-5, the stiffness of the specimen was constant until about 18-kips. After this point the specimen maintained its stiffness until approximately 27-kips where the stiffness reduced significantly. Again, the concrete below the hole cracked at either end and fell out. There did not appear to be any anchorage problems in the performance of the specimen

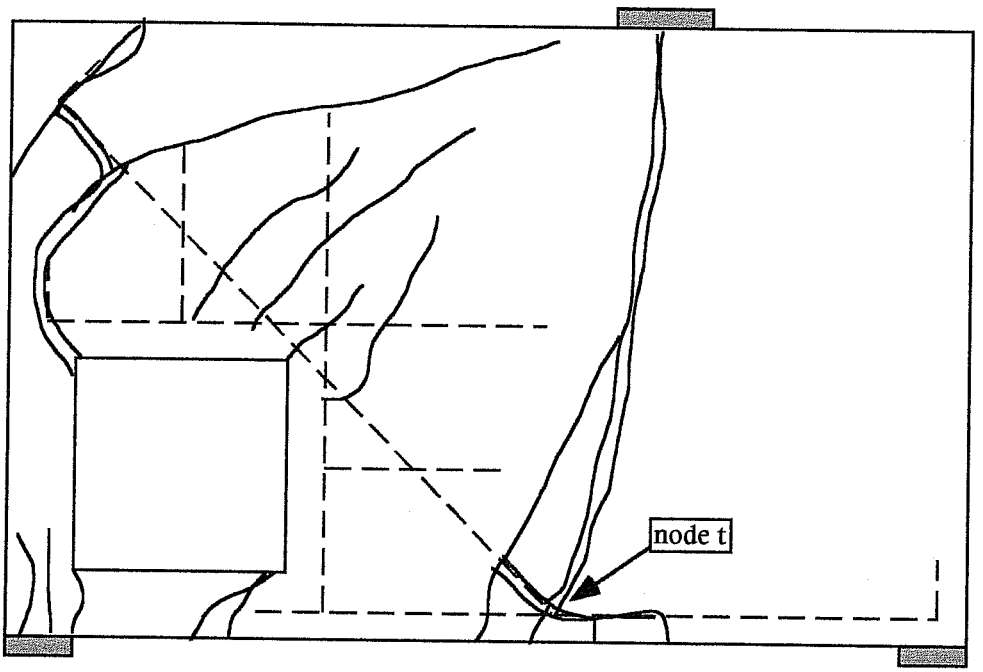

A.) Cracking Pattern

B.) Photograph of Cracking Pattern

Figure 7-3 - Cracking Pattern for Specimen 3

7.5. Specimen 4

7.5.1. Specimen Performance and Results

Specimen 4 differed from Specimen 3 only in the extra reinforcement placed below the hole. Specimen 4 contained 8.5-lbs. of steel and withstood an ultimate load of 43-kips. This specimen experienced its first crack at 20-kips when a crack formed at 45-degrees from the upper right corner of the hole. The two 6-mm bars below the hole prevented a crack from forming below the hole early in the loading. A crack did finally form at the lower left corner of the hole at 28-kips. At 35-kips, the lower right corner of the deep beam failed in bearing.

Again, due to this premature localized bearing failure, the integrity of the strut-and-tie model could not be properly evaluated. Thus, the lower corner was repaired using epoxy and the support moved in to give a larger bearing area. The specimen was reloaded yielding a load-deflection curve shown in Figure 7-5. During the reloading, new cracks started to form at 28-kips on the right side of the specimen. Spalling occurred again at the right support but stopped soon after. At 36-kips and 38-kips a large shear crack formed from the column to the load. This crack continued to grow until failure. Again at 42-kips the column started to crush near the support.

All cracks are shown in Figure 7-4. On the right side of the specimen the cracks stopped growing at 28-kips. At 40-kips, the beam failed in flexure and shear. The concrete below the hole split away from the two reinforcing bars as the bars stretched and started to fail in anchorage at the left hook. The entire area surrounding the steel in the upper left part of the specimen failed in compression and tension.

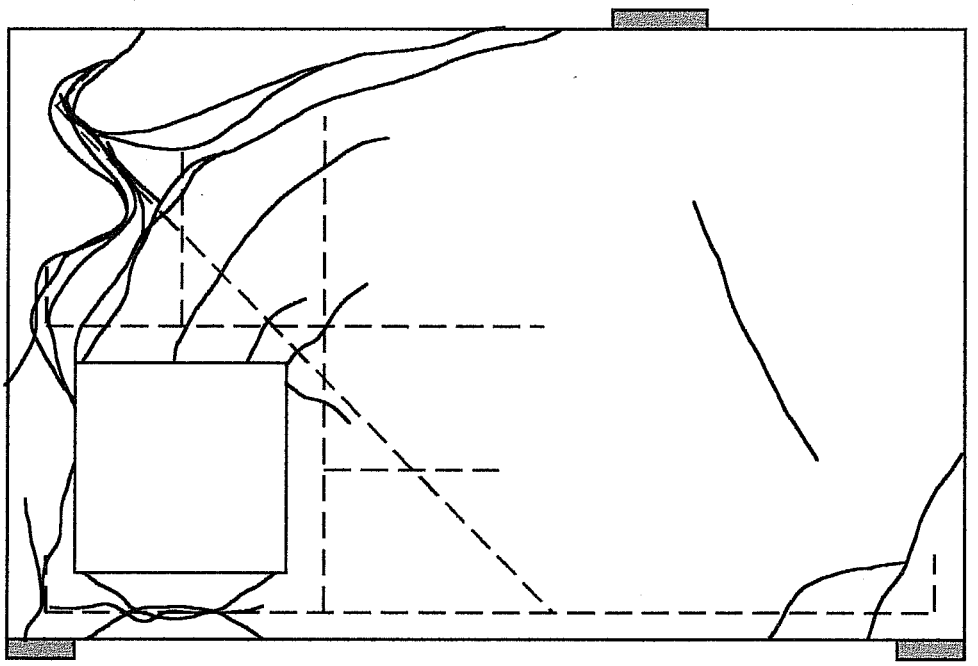

A.) Cracking Pattern

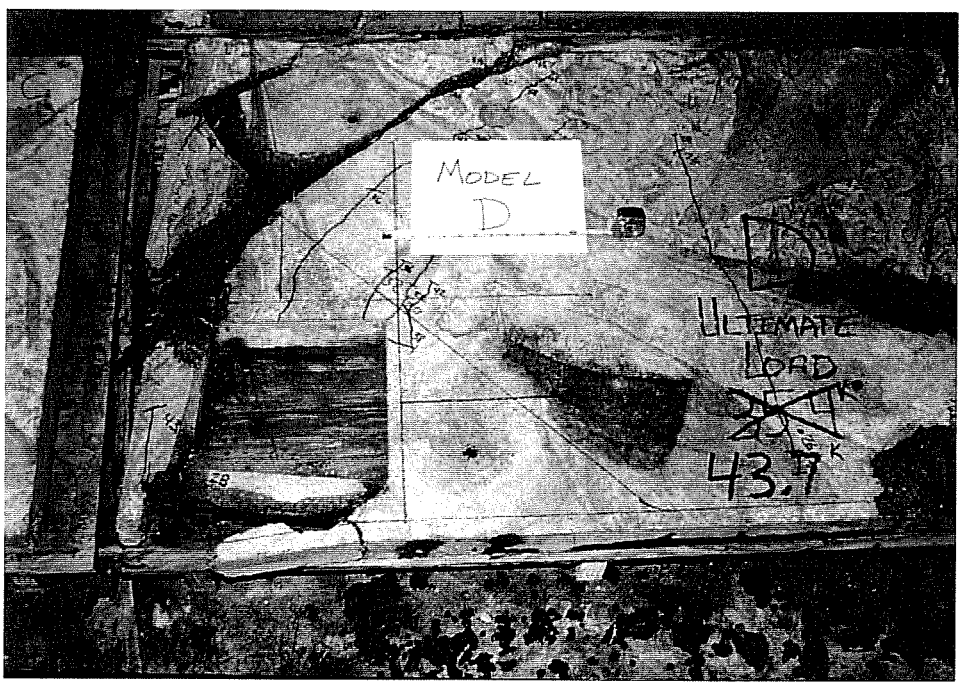

B.) Photograph of Cracking Pattern

Figure 7-4 - Cracking Pattern for Specimen 4

7.6. Conclusion

Overall, the four specimens performed very well in relation to the factored design load of 22-kips. All four specimens carried loads in excess of the factored design loads, thus showing the conservatism of the strut-and-tie model technique. The results from all of the specimens are given in Table 7-1. The ultimate load and deflection at the factored design load are given along with the concrete strength and weight of steel. Figure 7-5 shows the load versus deflection curves for all four specimens. Thus all results are shown, and evaluation and analysis of these results will be presented in the next chapter.

Table 7-1 - Test Results for All Specimens

Specimen	fc (psi.)	Weight of Steel Used (lbs.)	Deflection at 22-kips (in.)	Ultimate Load Pu (kips)
1	4170	8.9	0.124	31
2	4020	5.3	0.131	33
3	4040	7.6	0.113	41
4	4160	8.5	0.111	43

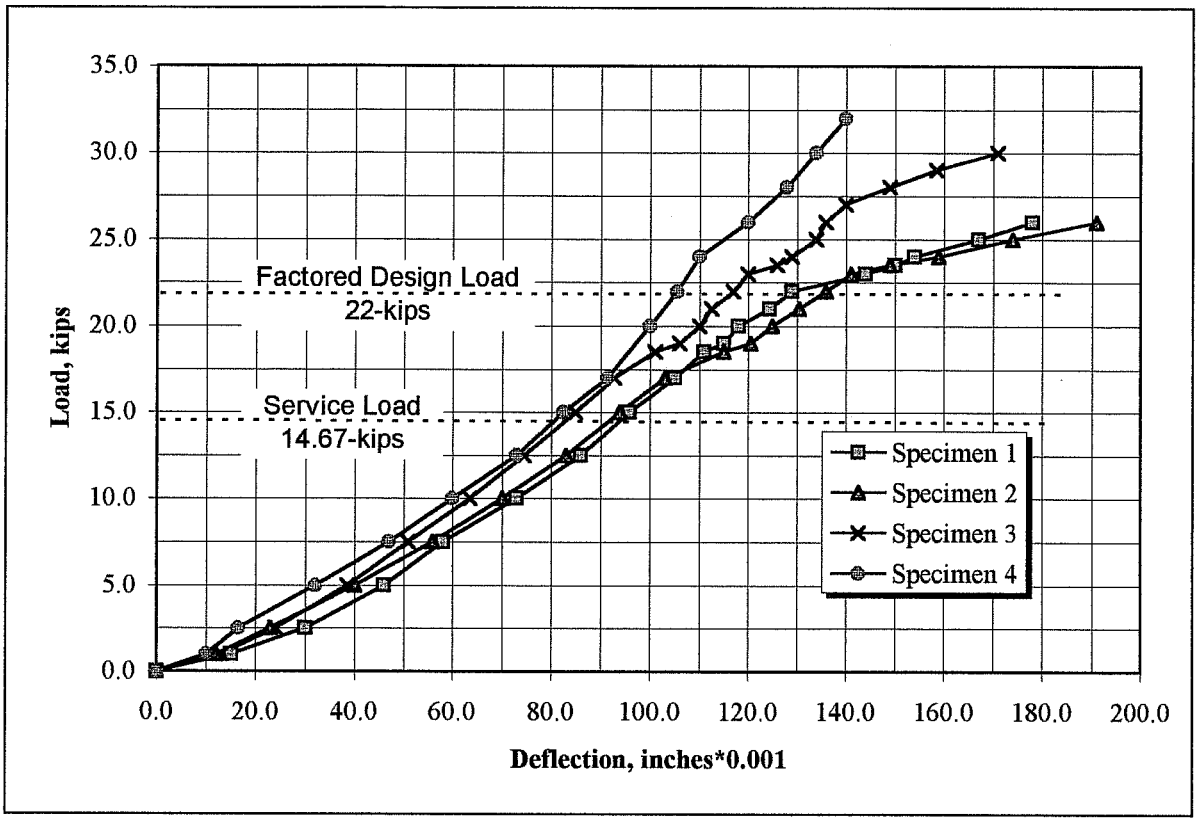

Figure 7-5 - Load versus Deflection Curves for All Specimens

CHAPTER 8

DISCUSSION OF ANALYTICAL AND EXPERIMENTAL RESULTS

8.1. Introduction

Overall, the performance of the four strut-and-tie model specimens exceeded expectations thus verifying the usefulness of the strut-and-tie modeling technique. Each specimen carried more than the factored design load of 22-kips. All specimens experienced small deflections with few cracks at the factored design load. The specimens performed well from a serviceability viewpoint also. The service load or unfactored load was 14.67-kips and at this load the specimens were not visibly cracked. The strength of the four deep beams conservatively ranged from fifty to one hundred percent more than the factored design load. The development length tests performed using the small bars and microconcrete and the design values based on these tests proved successful as the specimens experienced no anchorage failures. The limiting factor in all cases was the deterioration of the concrete at high load levels.

This chapter will examine all experimental test results and compare the results to analytical design expectations. The success and significance of the tests are explored. Furthermore, changes needed and problems experienced during testing are discussed.

8.2. Analysis of Experimental Test Results

It is important to examine the test results, failure load, and crack patterns of the four specimens to characterize the behavior of the strut-and-tie model specimens. Based on the data presented in Chapter 7, a number of conclusions can be made. The experimental results

show how the failure mechanism of one specimen is corrected in another specimen which fails at a new weakness.

Specimen 1 ultimately failed in shear as shown in Figure 8-1. A large crack formed above the top of the bars which ran vertically above the hole. This crack split the area of unreinforced concrete in the upper left part of the specimen. This shear failure mode was eliminated in Specimens 2 and 3 by extending bars through the shear failure region. These bars helped avoid the shear failure, and the shear crack did not form in Specimen 2 and 3. However, the even higher loads of Specimen 4 did cause the shear crack to reappear. Another area of interest in Specimen 1 is where the horizontal bars anchor above the left side of the opening. This region is highly stressed and was a weak point for Specimens 1, 3, and 4.

Specimen 2 ultimately failed due to flexural forces as seen in Figure 8-1. The bent reinforcing bars extended almost to the top of the beam precluding a shear failure. The bars strained as the beam was stressed in tension across the corner. The concrete below the strained reinforcing bars was destroyed and fell away. This specimen was the most flexible and experienced the greatest deflection although it was stiffer than Specimen 1 for low loads. Referring to Figure 7-5, Specimen 2 initially had a greater stiffness than Specimen 1, but degraded at higher load levels. Specimen 2 split perpendicular to the reinforcing bars due to the flexural forces, but ultimately held fifty percent more than the design load. This specimen performed the poorest because it had the largest cracks and deflection. The overall strut-and-tie model would probably be considered poor because it contains a very long tie member. Schlaich et al. point out that the model with the fewest and shortest ties is the best (1987).

Specimen 3 is a combination of the strut-and-tie models used in Specimens 1 and 2. A shear crack formed as in Specimen 1, but the reinforcing bars placed at a 45-degree angle

passed through the crack and stopped its growth. Crack patterns for all specimens are shown in Figure 8-1. The horizontal and vertical steel resisted a flexural failure like that of Specimen 2, and instead, the specimen experienced a flexural failure at the bottom node where the longitudinal bars bend to angle up across the hole. The beam's flexural forces caused the concrete below this node to crack and eventually fall away. A severe crack formed straight down from the loading point to the lower node. This crack ran alongside the right side steel mesh. Also, there were problems with transferring load from the left hooked ends of the horizontal bars above the opening into the column, and the column crushed at the support under the high load.

In contrast, due to the added benefit of the reinforcing steel placed under the opening, Specimen 4 did not fail in the same manner as Specimen 3. The extra longitudinal bars placed beneath the hole strengthened the beam and precluded flexural problems. For Specimen 4, the failure mechanism was a shear failure. There was severe degradation of the concrete around the left end of the bent reinforcing bar, and the bars at the bottom of the deep beam beneath the hole experienced large flexural forces. On the left end of the horizontal bars placed below the hole, the anchorage hooks pulled out of the column which degraded the column at the support. The column on the left of the opening performed the worst in this specimen. Specimen 4 was the stiffest of all specimens as the flexural steel did not allow the beam to deflect much. This specimen carried nearly double the design load.

The concrete below the opening performed poorly as expected for Specimens 1, 2, and 3. There was no reinforcing steel below the opening in these specimens. In all cases, the first crack appeared as a vertical crack originating from the lower left corner of the opening, and, as the test proceeded, the concrete below the hole cracked at the other end and fell away.

Again, this was expected and the load capacity of the beam was not affected. The fourth specimen was designed to compensate for this problem by adding reinforcement below the hole. Successfully, this extra reinforcement prevented any crack from forming at the factored design load, and caused the beam to fail in shear at a high load level instead of a flexural failure.

In all specimens, there was no failure in the concrete and steel mesh on the right side of the specimens. In only the fourth specimen did any cracks form in that region, and in that case, the crack appeared but did not continue to grow. There was more than enough reinforcement on the right side of the specimen, and the concrete did not fail.

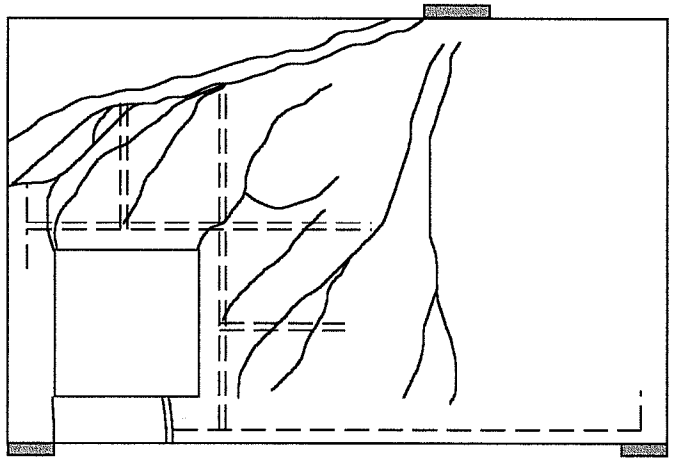

A.) Specimen 1 P_u = 31-kips

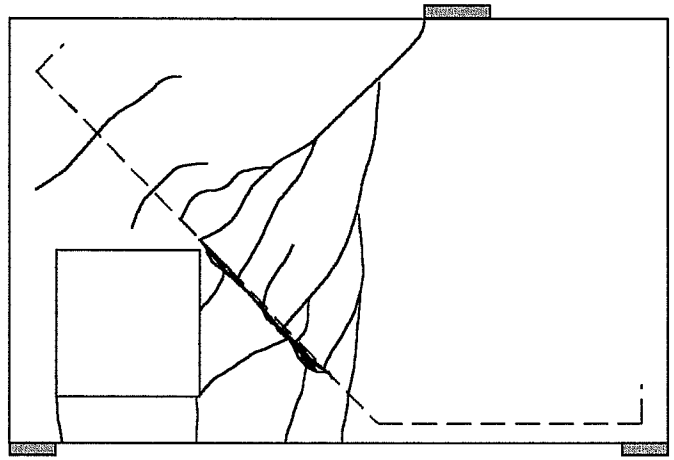

B.) Specimen 2 P_u = 33-kips

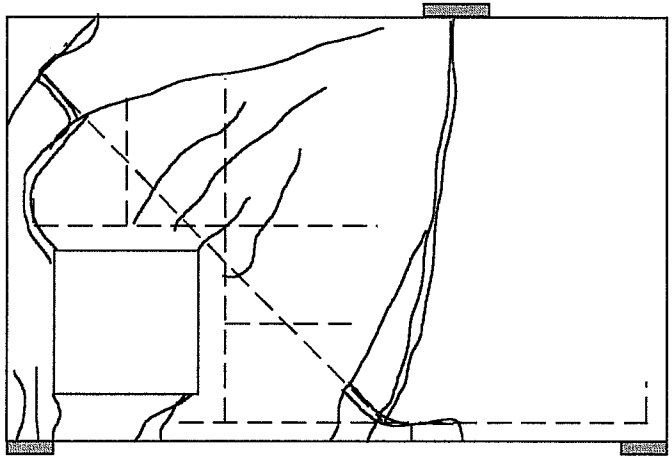

C.) Specimen 3 P_u = 43-kips

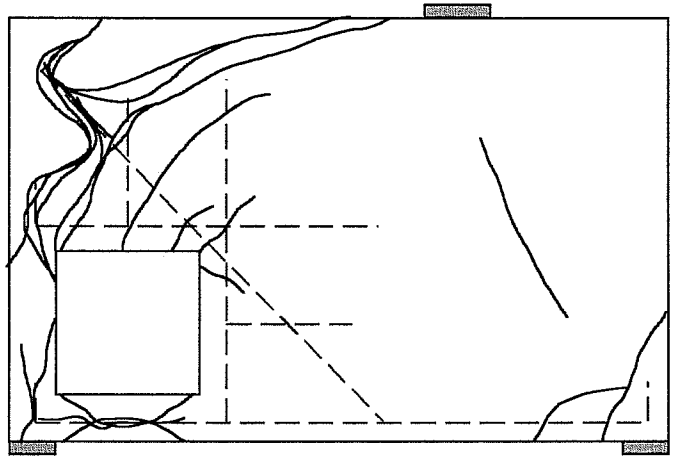

D.) Specimen 4 P_u = 41-kips

Figure 8-1 - Cracking Patterns

8.3. Significance of Results

The excellent performance of the four deep beam specimens experimentally demonstrates the reliability and conservatism of the strut-and-tie model. The results also show failure mechanism differences among the four specimens. If one specimen fails in shear, fixing the problem caused the next specimen to fail differently, perhaps in flexure, and always at a higher load level.

From an economy viewpoint, the second specimen was best because it used the least amount of steel, but still carried the factored design load. However, if the specimen was full-sized, the number of splices and the bending of the bars necessary may pose a threat to the constructability of the overall deep beam. From a constructability viewpoint, the first specimen would be best. No special procedures would be needed to construct the reinforcement cage.

8.5. Limitations of the Solution

Limitations in the design exist due to the tight scope of the investigation. Since the purpose of the experiment was to test the strut-and-tie model performance, extra steel normally used for serviceability, crack control, and shrinkage control was ignored. Overall, however the performance of the specimens can and should be classified as outstanding.

8.5.1. Problems in the Project and the Corresponding Solutions

The biggest problem in this investigation occurred during testing. The phenomenon of local bearing failure was not accounted for in design because it was not seen as a possible problem. However, the first specimen experienced a bearing failure at the load point and a larger loading pad was needed to eliminate bearing failure in this and other specimen tests. A

spiral of reinforcement steel should have been placed directly beneath the loading point to solve any bearing failure problems.

8.5.2. Changes Needed In the Investigation

Change in future investigations of this type is needed in the area of improving the concrete quality. Due to the restricted funds of this investigation, pre-bagged concrete mix was used and mixed with a superplasticizer to create an acceptable concrete. While this concrete did perform as expected, the time and labor involved in using this material was large. Further, the quality of the concrete was questioned because some of the samples seemed to be quite sandy. Further changes also need to occur in tying the reinforcement bars together. Small wooden blocks were used to hold the bars in position, and these blocks were probably too large, possibly hindering the performance of the specimens. Smaller bar supports should be used

8.6. Conclusions

The performance of the specimens was outstanding. This chapter examined how each specimen failed and how the investigation could be improved. However, it is very important to remember that each specimen performed extremely well at the factored design load. Deflections at the factored design load were around L/400 and even less at service load levels as seen in Figure 7-5. Each specimen had far more than the required strength to carry factored design loads. The weakest of the beams held fifty percent more load than required. Cracks had formed at the factored design load, but no visible cracks formed at service level loads. Design improvements are possible and further research needed, but overall, the strut-and-tie modeling technique and the specimens performed well.

CHAPTER 9

CONCLUSION

9.1. Brief Summary

Where geometric discontinuities exist in structural concrete members, current code documents provide little direction for design. A greater understanding of how to design a reinforced concrete deep beam with a geometric discontinuity in the form of a large opening can be obtained by using strut-and-tie models. Combinations of two distinctly different strut-and-tie models were used to design four specimens. Physical models were constructed using sack concrete and 3-mm and 6-mm reinforcing bars. The development lengths for the small bars were determined using a method developed by Ferguson at The University of Texas. The deep beams were simply supported and tested using a point load. Each of the four beams resisted considerably more than the factored design load. This successful test series reveals the power, versatility, reliability, and predictability of the strut-and-tie modeling technique.

9.2. Conclusions

The question posed in the first chapter of how to consistently design reinforced concrete members with discontinuities is answered by the strut-and-tie modeling technique. Previous authors have developed and investigated the strut-and-tie model, and the focus of this paper was to experimentally test their ideas on a fairly complex specimen. This investigation successfully verified their ideas. Specific conclusions made from this study are:

1) Strut-and-tie models provide lower bound design solutions that are valid, conservative, and reliable for the deep beam investigated.
2) Using two strut-and-tie models for the design of one specimen, each proportioned to carry half of the factored design load, provided a beneficial redundancy which yielded a stiffer and stronger deep beam.
3) The performance of the deep beam specimens at the factored design load of 22-kips was very good. Each specimen was much stronger than the factored design load and at this load there was very little deflection and few cracks.
4) The performance of the deep beams at the service load of 14.67-kips was excellent. None of the specimens developed visible cracks at service loads and deflections were very small.
5) The failure mechanism of the initial specimen was corrected in the next specimen which failed at a new weakness. In this way, differences between the failure patterns were observed and an improved solution can be developed.
6) The development length tests performed using the small reinforcing bars and the microconcrete mix were very important in the design. By knowing the properties of these scaled materials, it was possible to prevent any anchorage problems that might occur in the deep beam specimens.
7) Local bearing failure is a problem that needs to be addressed and prevented in the design of the specimens. The steel needed to prevent bearing failure is inexpensive and easy to install and should be used.

9.3. Factors Leading To Success In the Overall Investigation

As with any project, success depends on a number of different and widely varied factors. In the case of this investigation, the success of the specimens is primarily due to the previous design work done by Schlaich et al. Their design functioned as a spring board for this investigation. Another area that led to the success of this project was the work done to determine the development lengths of the small bars in the microconcrete. By knowing the unique nature of the scale materials, a proper design was accomplished. Other than that, success is credited to careful constructing, casting, and testing of the specimens.

9.4. Recommendations for Further Research

Further research on these same type of deep beam specimens needs to be conducted to include reinforcement for creep, shrinkage, and crack control. Research could be used to test larger specimens using a high quality concrete. The concrete used should be of similar quality available in everyday construction. Standard reinforcement bars could also be used with these larger specimens. These larger specimen tests could be useful in determining any additional problems, but overall the strut-and-tie modeling technique gives the designer direction in unique design problems.

REFERENCES

ACI Committee 318 (1995) "Building Code Requirements for Structural Concrete (ACI 318-95 / ACI 318R-95)." American Concrete Institute, Detroit, Michigan.

Aldridge, W. W. (June 1966) "Ultimate Tests of Model Reinforced Concrete Folded Plate Structures." Dissertation, The University of Texas, Austin, Texas.

Bergmeister, K., Breen, J. E., Jirsa, J. O., and Kreger, M. E. (1993) "Detailing for Structural Concrete." Research Report 1127-3F. Center for Transportation Research, The University of Texas at Austin, Austin, Texas.

Ferguson, P. M., Breen, J. E., and Jirsa, J. O. (1988) *Reinforced Concrete Fundamentals.* John Wiley and Sons, New York, New York.

Ferguson, P. M. and Thompson, J. N. (July 1962) "Development Length of High Strength Reinforcing Bars in Bond." *ACI Journal*, Vol. 59, No. 7, pp 887-992.

Schlaich, J., Shäfer, K., and Jennewein, M. (1987) "Toward a Consistent Design of Structural Concrete." *PCI Journal*, Special Report, Vol. 32, No. 3, pp 74-150.

Waxler, Ronnie (June 3, 1996) Telephone interview. TXR Industries, Austin, Texas.